Climate Hazard Assessment for Stakeholder Adaptation Planning In New York City

Radley M. Horton[*], Vivien Gornitz[*], Daniel A. Bader[*], Alex C. Ruane[+,*], Richard Goldberg[*], and Cynthia Rosenzweig[+,*]

[*] Center for Climate Systems Research, Earth Institute, Columbia University, New York, NY

[+] NASA Goddard Institute for Space Studies, New York, NY

***Corresponding author address*: Radley Horton, Columbia University Center for Climate Systems Research, 2880 Broadway, New York, NY, 10025.**

Email: rh142@columbia.edu

Abstract

This paper describes a time-sensitive approach to climate change projections, developed as part of New York City's climate change adaptation process, that has provided decision support to stakeholders from 40 agencies, regional planning associations, and private companies. The approach optimizes production of projections given constraints faced by decision makers as they incorporate climate change into long-term planning and policy. New York City stakeholders, who are well-versed in risk management, helped pre-select the climate variables most likely to impact urban infrastructure, and requested a projection range rather than a single 'most likely' outcome. The climate projections approach is transferable to other regions and consistent with broader efforts to provide climate services, including impact, vulnerability, and adaptation information.

The approach uses 16 Global Climate Models (GCMs) and three emissions scenarios to calculate monthly change factors based on 30-year average future time slices relative to a 30-year model baseline. Projecting these model mean changes onto observed station data for New York City yields dramatic changes in the frequency of extreme events such as coastal flooding and dangerous heat events. Based on these methods, the current 1-in-10 year coastal flood is projected to occur more than once every 3 years by the end of the century, and heat events are projected to approximately triple in frequency. These frequency changes are of sufficient magnitude to merit consideration in long-term adaptation planning, even though the precise changes in extreme event frequency are highly uncertain.

1. Introduction

This paper describes a methodological approach to stakeholder-driven climate hazard assessment developed for the New York Metropolitan Region (Fig. 1). The methods were developed in support of the New York City Panel on Climate Change (NPCC; NPCC 2010). The NPCC is an advisory body to New York City's Climate Change Adaptation Task Force (CCATF), formed by Mayor Michael Bloomberg in 2008 and overseen by the Mayor's Office of Long Term Planning and Sustainability. As described in NPCC (2010), the CCATF is comprised of stakeholders from 40 city and state agencies, authorities, regional planning associations, and private companies, divided into four infrastructure workgroups (communication, energy, transportation, and water and waste), and one policy workgroup.

The CCATF effort was motivated by the fact that New York City's population and critical infrastructure are exposed to a range of climate hazards, with coastal flooding associated with storms and sea level rise the most obvious threat. Approximately 7 % (11%) of NYC area is within 1 meter (2) of sea level (Weiss et al. 2011). A recent study ranked NYC 7th globally among port cities in exposed population and 2nd globally in assets exposed to storm surge flooding and high winds (Nicholls et al. 2008). Furthermore, because NYC, like much of the U.S. (ASCE, 2009), has aging infrastructure, climate vulnerability may be enhanced. By showing leadership in the infrastructure adaptation process, the NYC effort may be able to provide lessons to other cities as they plan adaptation strategies.

Stakeholder input regarding climate information was collected in several ways. Between September of 2008 and September of 2009, each CCATF sector working group held monthly meetings in conjunction with the Mayor's Office of Long Term Planning and Sustainability. During the initial meetings, representatives from each sector identified key climate hazards; they

63 also interacted iteratively with the scientists, seeking clarification, and requesting additional
64 information. They commented on draft documents describing the region's climate hazards, and
65 climate seminars were held with individual agencies as requested. The climate hazard
66 assessment process was facilitated by prior collaborative experience between the NPCC's
67 climate scientists and stakeholders in earlier assessments, including the Metro East Coast Study
68 (MEC; MEC 2001), as well as work with the New York City Department of Environmental
69 Protection (NYCDEP; NYCDEP 2008; Rosenzweig et al. 2007) and the Metropolitan Transit
70 Authority (MTA; MTA 2007).

71 The climate hazard approach is tailored towards impact assessment; it takes into
72 consideration the resource and time constraints faced by decision makers as they incorporate
73 climate change into their long-term planning. For example, the formal write-up of the climate
74 risk information was needed within less than 8 months of the NPCC's launch (NRC 2009); given
75 this time frame and the broad array of stakeholders in the CCATF, a standardized set of climate
76 variables of broad interest were emphasized, with the understanding that future studies could
77 provide climate information tailored to more unique applications[1].

78 Within this framework, the NPCC worked with stakeholders to pre-select for analysis
79 climate variables and metrics most likely to impact existing assets, planned investments, and
80 operations (Horton and Rosenzweig 2010). For example, the number of days below freezing was
81 identified as an important metric for many sectors, due to the impacts of freeze-thaw cycles on
82 critical infrastructure (New York City Climate Change Adaptation Task Force, 2008-2009). Due

[1] A tailored assessment of changes in snow depth and timing of snow melt in the Catskill Mountains approximately 100 miles north of New York City (NYC DEP, 2008) would be of interest to managers of only a small but important subset of infrastructure—reservoirs and water tunnels. Such a fine-scale assessment would benefit from more complex downscaling approaches than those applied here.

to the diversity of agencies, projections were requested for multiple time periods spanning the entire 21st century.

Stakeholders also helped determine the presentation of climate hazard information. For example, because NYC stakeholders are used to making long-term decisions under uncertainty associated with projections of future revenues, expenditures, and population trends, for example, they preferred projection ranges to a single 'most likely' value (New York City Climate Change Adaptation Task Force, 2008-2009).

Itemized risks associated with each climate variable were ultimately mapped to specific adaptation strategies. For example, more frequent and intense coastal flooding due to higher mean sea level was linked to increased seawater flow into New York City's gravity-fed and low-lying Wastewater Pollution Control Plants (WPCP), resulting in reduced ability to discharge treated effluent (NPCC 2010; NYCDEP 2008). NYCDEP is reducing the risk at the Far Rockaway Wastewater Treatment Plant by raising pumps and electrical equipment to 14ft above sea level based on the projections described here (NYC Office of the Mayor, 2009).

Climate hazard assessment was only one component of the NPCC's impact and adaptation assessment. Vulnerability of infrastructure (and the populations that rely on it) to climate impacts can be driven as much by its state of repair (and how it is used) as by climate hazards (NRC, 2009). Climate adaptation strategies should be based on many non-climate related factors, such as co-benefits (e.g., some infrastructure investments that reduce climate risks will also yield more efficient and resilient infrastructure in the face of non-climate hazards; NRC 2010a) and co-costs (e.g., adapting by using more air conditioning increases greenhouse gas emissions). NPCC experts in the risk management, insurance, and legal fields provided guidance on these broader issues of vulnerability and adaptation, developing for example an eight step

adaptation assessment process and templates for ranking relative risk and prioritizing adaptation strategies (NPCC, 2010). This paper focuses on the provision of stakeholder-relevant climate information in support of the broader NPCC assessment.

Section 2 describes the methodology used for the NPCC's climate hazard assessment. Section 3 compares climate model hindcasts to observational results for the New York Metropolitan Region. Hindcast results are a recurring stakeholder request, and they helped inform the global climate model (GCM)-based projection methods. Section 4 documents the regional projections, in the context of stakeholder usability. Section 5 covers conclusions and recommendations for future work.

2. Methodology

a. Observations

Observed data are from two sources. Central Park station data from the National Oceanic and Atmospheric Administration, National Climatic Data Center, United States Historical Climatology Network (NOAA NCDC USHCN) Version 1 data set (Karl et al. 1990; Easterling et al. 1999; Williams et al. 2005) formed the basis of the historical analysis and projections of temperature and precipitation. Gridded output corresponding to New York City from the National Centers for Environmental Prediction / Department of Energy (NCEP/DOE) Reanalysis 2 output (Kanamitsu et al. 2002) is also used for GCM temperature validation (section 3).

b. Climate Projections: General Approach

1) GLOBAL CLIMATE MODELS AND EMISSIONS SCENARIOS

128 Climate projections are based on the coupled GCMs used for the Intergovernmental Panel
129 on Climate Change Fourth Assessment Report (IPCC; IPCC, 2007). The outputs are provided by
130 the World Climate Research Programme's (WCRP's) Coupled Model Intercomparison Project
131 phase 3 (CMIP3) multi-model dataset (Meehl et al. 2007a). Out of 23 GCM configurations from
132 16 centers, the 16 GCMs that had available output for all three emissions scenarios archived by
133 WCRP were selected (Table 1; A2, A1B, and B1; IPCC Special Report on Emissions Scenarios;
134 SRES; Nakicenovic et al. 2000).

135 The 16 GCMs and three emissions scenarios combine to produce 48 output sets. The 48
136 members yield a model and scenario-based distribution function based on equal weighting of
137 each GCM and emissions scenario. The model-based results should not be mistaken for a
138 statistical probability distribution (Brekke et al. 2008) for reasons including the following: 1) no
139 probabilities are assigned by the IPCC to the emissions scenarios[2] 2) GCMs are not completely
140 independent; with many sharing portions of their code and a couple differing principally in
141 resolution only, and 3) the GCMs and emissions scenarios do not sample all possible outcomes,
142 which include the possibility of large positive ice-albedo and carbon cycle feedbacks, in addition
143 to uncertain aerosol effects. Caveats notwithstanding, the model-based approach has the
144 advantage (relative to projections based on single numbers) of providing stakeholders with a
145 range of possible outcomes associated with uncertainties in future greenhouse gas concentrations
146 (and other radiatively important agents and climate sensitivity (NRC, 2010b).

147 Some authors (see e.g., Smith et al. 2009; Tebaldi et al. 2005; Greene et al. 2006; Brekke

[2] It has been argued that since high global anthropogenic CO_2 emissions growth rates (3.4 % $year^{-1}$ between 2000 and 2008; Le Quere et al. 2009) led to 2008 estimated emissions reaching the levels of the highest SRES scenario (A1FI), other SRES scenarios may be unrealistically low.

et.al. 2008; Georgi and Mearns 2002) have explored alternate approaches that weight GCMs based on criteria including hindcasts of regional climate or key physical processes. That more complex approach is eschewed here in favor of equal GCM weighting for several reasons. First, because model 'success' is often region and variable-specific, and stakeholders differ in their climate variables and geographical ranges of interest[3], production of consistent scenarios based on model weighting is a major research effort beyond the scope of New York City's initial assessment. Second, while long-term research could be geared towards developing optimized multivariate (and/or multi-region) weighting, research suggests that compensating biases tend to yield comparable model performance (Brekke et al. 2008). Third, historical accuracy may have been achieved for the 'wrong' reasons (Brekke et al. 2008) and GCM hindcasts did not share identical forcing, especially with respect to aerosols (Rind et al. 2009). Fourth, shifting climate processes with climate change may favor different models in the future. Finally, eliminating ensemble members reduces the representation of uncertainty relating to climate sensitivity.

2) TIMESLICES

Because current-generation GCMs used for climate change applications have freely evolving ocean and atmospheric states, they are most appropriate for detection of long-term climate and climate change signals. The 30-year timeslice applied here is a standard timescale (WMO 1989) that represents a middle ground, allowing partial cancellation of currently unpredictable interannual to interdecadal variability (maximized by including many years), while maintaining relatively monotonic anthropogenically-induced forcing trends (maximized by including few years). The '1980s' timeslice represents baseline conditions between 1970-1999;

[3] New York City's task force included corporations with national and international operations.

170 future timeslices for the 2020s, 2050s, and 2080s are similarly defined.

171

172 ### 3) CLIMATE CHANGE FACTORS AND THE DELTA METHOD

173 Mean temperature change projections are expressed as differences between each model's
174 future timeslice simulation and its baseline simulation; mean precipitation is based on the ratio of
175 a given model's future to its baseline values. This approach offsets a large source of model bias:
176 poor GCM simulation of local baseline conditions (section 3b) arising from a range of factors
177 including the large difference in spatial resolution between GCM gridboxes and station data.

178 Because monthly averages from GCMs are generally more reliable than daily output
179 (Grotch and MacCracken 1991), monthly mean GCM changes were projected onto observed
180 1971-2000 daily Central Park data for the calculation of extreme events[4]. This simple and low-
181 cost downscaling approach is known as the delta method (Gleick 1986; Arnell 1996; Wilby et al.
182 2004). Like more complex statistical downscaling techniques (e.g., Wigley et al. 1990), the delta
183 method is based on stationarity (see e.g., Wilby et al. 1998 and 2002; Wood 2004), and largely
184 excludes the possibility of large variance changes through time, although for the Northeast U.S.
185 such changes are uncertain[5].

186 More complex statistical approaches, such as those that empirically link large-scale
187 predictors from a GCM to local predictands (see e.g., Bardossy and Plate 1992) may yield more
188 nuanced downscaled projections than the delta method. These projections are not necessarily

[4] For coastal flooding and drought, the 20th century was used as a baseline, due to high interannual/multidecadal variability and policy-relevance of 1-in-100 year events.

[5] An exception may be short-term precipitation variance, which is expected to increase regionally with the more intense precipitation events associated with a moister atmosphere (see e.g., Emori and Brown 2005; Cubasch et al. 2001; Meehl et al. 2005)

189 more realistic, however. Historical relationships between large-scale predictors and more
190 impacts-relevant local predictands may not be valid in a changing climate (Wilby et al. 2004).
191 GCM development and evaluation has also historically been more focused on seasonal and
192 annual climatologies than the daily and interannual distributions that drive analogue approaches.
193 Table 2 provides a set of stakeholder questions to inform the choice of downscaling technique, a
194 topic that is discussed further in Section 5.
195
196 4) SPATIAL EXTENT
197 The projections are for the land-based GCM gridbox covering New York City. As shown
198 in Fig. 2, the 30-year averaged mean climate changes are largely invariant at sub-regional scales;
199 the single grid box approach produces nearly identical results to more complex methods that
200 require extraction of data from multiple gridboxes and weighted spatial interpolation. As shown
201 in section 4e, for the metrics evaluated in this study, the GCM gridbox results also produce
202 comparable results to finer resolution statistically and dynamically downscaled products. Since
203 baseline climate (as opposed to projected climate change) does differ dramatically over small
204 spatial scales (due to factors such as elevation and surface characteristics), and these fine-scale
205 spatial variations by definition cannot be captured by course-resolution GCMs, GCM changes
206 are trained onto observed Central Park data using the procedures described above.
207
208 5) NUMBER OF SIMULATIONS
209 For 13 of the 16 GCMs' Climate of the 20th Century and future A1B experiments, and 7
210 of the 16 B1 and A2 future experiments, multiple simulations driven by different initial
211 conditions were available. Analysis of hindcasts (Table 3a) and projections (Table 3b) from the

212 available NCAR CCSM coupled GCM simulations[6] revealed only minor variations in 30-year
213 averages, suggesting that one simulation per model is sufficient. Using an ensemble for each
214 GCM based on all the available simulations with that GCM is an alternative approach; however,
215 the effort and data storage needs may not be justified given the similarity of the ensemble and
216 individual simulation results shown in Table 3. Furthermore, ensemble averaging unrealistically
217 shrinks the temporal standard deviation[7].
218
219 *c. Climate Projections: Sea Level Rise*
220 To address large uncertainties associated with future melting of ice sheets, two sea level
221 rise projection methods were developed: these are referred to as the IPCC-based and rapid ice
222 melt scenarios respectively.
223
224 1) IPCC AR4-BASED APPROACH
225 The IPCC Fourth Assessment (AR4) approach (Meehl et al. 2007b) was regionalized for
226 New York City utilizing four factors that contribute to sea level rise: global thermal expansion,
227 local water surface elevation, local land uplift/subsidence, and global meltwater[8]. Thermal
228 expansion and local water surface elevation terms are derived from the GCMs (outputs courtesy
229 of WCRP and Dr. Jonathan Gregory, personal communication). Local land subsidence is derived
230 from Peltier (2001) and Peltier's ICE-5Gv1.2 ice model (2007)
231 (http://www.pol.ac.uk/psmsl/peltier/index.html). The meltwater term was calculated using mass
232 balance temperature sensitivity coefficients for the different ice masses, based on observed

[6] This GCM was selected because it provided the most 20th and 21st century simulations
[7] This is a general criticism; for the particular case when the delta method is used (as here) shrinking of the temporal standard deviation has no bearing on the results
[8] Only seven GCMs provided outputs for sea level rise projections; see Horton and Rosenzweig (2010) for additional information.

233 historic relationships between global mean surface air temperature, ice mass, and rates of sea
234 level rise (Meehl et al. 2007b)[9]. Regionalization of sea level rise projections, based on the four-
235 components described above, have been used in other studies (e.g., Mote et al. 2008).
236
237 2) RAPID ICE MELT SCENARIO
238 Because of large uncertainties in dynamical ice sheet melting (Hansen et al. 2007; Horton
239 et al. 2008), and recent observations that ice sheet melting has accelerated within this past decade
240 (e.g., Chen et al. 2009), an alternative sea level rise scenario was developed. This upper bound
241 sea level rise scenario allowing for rapid ice melt was developed based on paleo-sea level
242 analogues, in particular the ~10,000-12,000-year period of rapid sea level rise following the end
243 of the last ice age (Peltier and Fairbanks 2006; Fairbanks 1989). While the analogue approach
244 has limitations (most notably, the continental ice supply is much smaller today; Rohling et al.
245 2008), past rapid rise is described below since it may help inform discussions of upper bounds of
246 future sea level rise.
247 Average sea level rise during this more than 10,000-year period after the last ice age was
248 9.9 to 11.9 cm decade^{-1}, although this rise was punctuated by several shorter episodes of more
249 rapid sea level rise. In the rapid ice-melt scenario, glaciers and ice sheets are assumed to melt at
250 that average rate. The meltwater term is applied as a second-order polynomial, with the average
251 present-day ice melt rate of 1.1 cm decade^{-1} for 2000-2004 used as a base. This represents the
252 sum of observed mountain glacier (Bindoff et al. 2007) and ice sheet melt (Shepherd and
253 Wingham 2007) during this period. The rapid ice-melt scenario replaces the IPCC meltwater
254 term with the modified meltwater term; the other three sea level terms remain unchanged. This

[9] Corrections were not made to account for reductions in glacier area over time.

255 approach does not consider how rapid ice melt might indirectly influence sea level in the New
256 York region through future second-order effects including gravitational, glacial isostatic
257 adjustments, and rotational terms (e.g. Mitrovica et al. 2001, 2009).
258
259 *d. Climate Projections: Extreme Events*
260 Based on stakeholder feedback, quantitative and qualitative projections were made using
261 the extreme events definitions stakeholders currently use. For example, temperature extremes
262 were defined based on specific thresholds, such as 90ºF (~32°C), that the New York City
263 Department of Buildings uses to define cooling requirements, whereas coastal flooding was
264 defined by frequency of occurrence (Solecki et al. 2010).
265
266 1) QUANTITATIVE PROJECTIONS: COASTAL FLOOD EXAMPLE
267 The coastal flooding projections are based on changes in mean sea level, not storms.
268 Projected changes in mean sea level (using the IPCC AR4-based approach) were superimposed
269 onto historical data. For coastal flooding, critical thresholds for decision-making are the 1-in-10
270 year, and 1-in-100 year flood events (Solecki et al. 2010). The latter metric is a determinant of
271 construction and environmental permitting, as well as flood insurance eligibility (Sussman and
272 Major 2010).
273 The 1-in-10 year event was defined using historical hourly tide data from the Battery tide
274 gauge, lower Manhattan (http://tidesandcurrents.noaa.gov; for more information, see Horton and
275 Rosenzweig 2010). The 1-in-100 year flood was analyzed using flood return period curves
276 based on data provided by the U.S. Army Corps of Engineers for the Metro East Coast Regional
277 Assessment (see Gornitz 2001 for details).

Because interannual variability is particularly large for rare events such as the 1-in-10 year flood, a base period of more than the standard 30 years was used. Similarly, since each year between 1962 and 1965 was drier in Central Park than the driest year between 1971 and 2000, the entire 20th century precipitation record was used for the drought analysis. More rigorous solutions for the rarest events await better predictions of interannual to multi-decadal variability, better understanding of the relationship between variability at those timescales and extreme events (see e.g. Namias 1966; Bradbury et al., 2002) and the growing event pool of realizations with time.

2) Qualitative extreme event projections

The question arose of how best to meet stakeholder needs when scientific understanding, data availability, and model output are incomplete; quantitative projections are unavailable for some of the important climate hazards consistently identified by infrastructure stakeholders and/or are characterized by such large uncertainties as to render quantitative projections inadvisable. Examples in the New York City region include ice storms, snowfall, lightning, intense sub-daily precipitation events, tropical storms and nor'easters. For these events, qualitative information was provided, describing only the most likely direction of change and an associated likelihood using the IPCC WG1 likelihood categories (IPCC, 2007)[10]. Sources of uncertainty and key historical events were also described, in order to provide stakeholders with

[10] Given the large impact of these extreme events on infrastructure, stakeholders requested information about likelihood for comparative purposes (e.g. "Which is more likely to increase in frequency? Nor'easters specifically, or intense precipitation events generally?"). Assignment of likelihood to generalized categories for qualitative extremes (based on published literature and expert judgment including peer review) was possible because predictions are general (e.g., direction of change),as opposed to the quantitative model-based projections.

297 context and the opportunity to assess sector-wide impacts of historical extremes.

298

299 3. GCM Hindcasts and Observations

300 The results of the GCM hindcasts and observational analysis described in this section
301 informed the development of the projection methods described in section two. Stakeholders
302 commonly request hindcasts and historical analysis (see e.g. NYCDEP 2008) as they provide
303 transparency to decision-makers who may be new to using GCM projections as a planning tool.

304

305 *a. Temperature and Precipitation Trends*

306 As shown in Table 4, both the observed and modeled 20th century warming trends at the
307 annual and seasonal scale are generally significant at the 99 percent level. While GCM 20th
308 century trends are generally approximately 50% smaller than the observed trends, it has been
309 estimated that approximately 1/3 of New York City's 20th century warming trend may be due to
310 urban heat island effects (Gaffin et al. 2008) that are external to GCMs. Over the 1970-1999
311 period of stronger greenhouse gas forcing, the observed annual trend was 0.21ºC decade^{-1}, and
312 the ensemble trend was 0.18ºC decade^{-1}.

313 Modeled seasonal warming trends in the past three decades and both annual and seasonal
314 precipitation trends over the entire century for New York City generally deviate strongly from
315 observations, consistent with prior results for the Northeast (see e.g. Hayhoe et al. 2007).
316 Observed and modeled trends in temperature and precipitation at a particular location are highly
317 dependent on internal variability, and therefore highly sensitive to the selection of years. For
318 example, the 1970-1999 observed Central Park annual precipitation trend of -1.77 cm decade^{-1}
319 shifts to 0.56 cm decade^{-1} when the analysis is extended through 2007. This is especially true for

the damaging extreme events[11] (Christensen et al. 2007) that are often of particular interest to infrastructure managers. In coupled GCM experiments with a freely evolving climate system, anomalies associated with climate variability generally will not coincide with observations, leading to departures between observed and modeled trends (Randall et al. 2007).

For stakeholders trained in analyzing recent local observations, it is challenging but important to emphasize that: 1) trends at continental and centennial timescales are often most appropriate for identifying the greenhouse gas signal and GCM performance, since (unpredictable) interannual to interdecadal variability is lower at those scales (Hegerl et al. 2007); and 2) during the 21st century, higher greenhouse gas concentrations and other radiatively important agents are expected to increase the role of the climate change signal, relative to climate variability.

b. Temperature and Precipitation Climatology

Comparison of station data to a GCM gridbox is hindered by the spatial scale discrepancy; New York City's low elevation, urban heat island (see e.g. Rosenzweig et al. 2006), and land sea contrasts are not captured by GCMs. As shown in Fig. 3a, the observed average annual temperature over the 1970-1999 period for New York City exceeds the GCM ensemble by 2.6ºC, and is higher than all but two of the 16 GCMs. When the GCMs are contrasted with the spatially comparable NCEP Reanalysis gridbox, the annual mean temperature bias is reduced

[11] Among 20th Century Central Park trends in observed extremes, only trends in cold extremes have been robust. For the number of days per year with minimum temperatures below freezing, both the 100-year trend of -2 days decade^{-1} and the 30-year trend of -5.2 days decade^{-1} are significant at the 99% level. GCM hindcasts of extreme events were not conducted due to the small signal to noise ratio.

339 to 1.1ºC. The departure of the Central Park station data from the GCM ensemble is largest in July
340 and smallest in January, indicating that the annual temperature cycle at this location is damped in
341 the GCMs (Fig. 3b**)**.

342 While Figure 3c reveals that the GCM ensemble of average annual precipitation from
343 1970-1999 is 8% below observations for Central Park, the ensemble average lies well within the
344 range of precipitation for New York City as a whole; GCM precipitation exceeds the LaGuardia
345 Airport station by 9%. Most of the GCMs are able to capture the relatively even distribution of
346 monthly precipitation throughout the year (Fig. 3d).

347 The above analysis reveals that mean climatology departures from observations over the
348 hindcast period are large enough to necessitate bias correction such as the delta method as part of
349 the GCM projection approach, rather than direct use of model output.

350

351 *c. Temperature and Precipitation Variance*

352 1) INTERANNUAL

353 Eleven (ten) of the 16 GCMs overestimate the 1970-1999 interannual standard deviation
354 of temperature, relative to the station data (NCEP reanalysis). The similarities between GCMs,
355 reanalysis and station data suggest that spatial-scale discontinuities may not have a large impact
356 on interannual temperature variance. All 16 GCMs underestimate interannual precipitation
357 variability relative to Central Park observations, and 14 of the 16 GCMs underestimate variance
358 relative to two other stations analyzed (Port Jervis and Bridgehampton). The large difference
359 between the GCMs and station data suggests that spatial-scale discontinuities, likely associated
360 with features like convective rainfall that cannot be resolved by GCMs, may be partially
361 responsible for the relatively low modeled interannual precipitation variance. Observed

362 interannual temperature variance is greatest in winter, a pattern not captured by seven on the 16
363 GCMs.
364
365 2) HIGH-FREQUENCY
366 The daily distribution of observed Central Park temperature (Fig.4 a-c) and precipitation
367 (Fig. 5) was compared to single gridbox output from 3 of the 16 GCMs used in the larger
368 analysis. The three models were part of a subset with daily output stored in the WCRP / CMIP3
369 repository and were selected because (of the subset) they featured the highest [Max Plank
370 Institute for Meteorology ECHAM5/MPI-OM (MPI, Jungclaus et al. 2005) and Commonwealth
371 Scientific and Industrial Research Organisation CSIRO-MK3.0 (CSIRO, Gordon et al. 2002),
372 both at 1.88ºlat. x 1.88ºlon.] and lowest [National Aeronautics and Space Administration
373 (NASA) / Goddard Institute for Space Studies (GISS) GISS-ER (GISS, Schmidt et al. 2006), at
374 4ºlat. x 5ºlon.] resolution. Analysis was conducted on summer (June-August) daily maximum
375 and winter (December-February) daily minimum temperature.
376 Summer maximum temperature distribution for the region in all three GCMs is narrower
377 than observations, and the warm tail is more poorly simulated than the cold tail. During winter,
378 CSIRO and MPI underestimate variance relative to the station data, while the GISS GCM has
379 excessive variance.
380 Figure 5 shows the number of days with precipitation exceeding 10 mm, a level of
381 rainfall that can trigger combined sewer overflow events at vulnerable sites in New York City
382 (PlaNYC 2008). Relative to Central Park data, all three GCMs underestimate the frequency of
383 daily precipitation above 50 mm--a level of precipitation that can lead to widespread flooding
384 and drainage problems including in subways (MTA 2007).

Given that precipitation in GCMs of this class and spatial resolution is highly parameterized to the gridbox spatial scale and seasonal/decadal climate timescales, departures of the distribution from observed daily station data can be expected. The low model variance at daily timescales for temperature and precipitation, and at interannual timescales for precipitation, reinforces the need for statistical downscaling approaches such as the delta method that apply monthly mean model changes to observed high frequency data.

d. Sea-Level Rise

Sea level was also hindcast for the 20th century, based on a 1990-1999 projection relative to the 1900-1904 base period.[12] The ensemble average hindcast is a rise of 18 cm, while the observed increase at the Battery is 25 cm. The five-year average local elevation term in the models meanders through time, frequently with an amplitude of 2-3 cm, with a maximum range over the century of approximately 7 cm, suggesting decadal variability (primarily in the local elevation term) and spatial resolution may explain the discrepancy between models and observations.

4. Future Projections

a. Mean Temperature and Precipitation

[12] In this calculation, the land subsidence term was identical to that used for the 21st century projections. The same surface mass balance coefficients used by the IPCC, based on global average temperature changes over a 1961-2003 baseline were used for the 1900-1904 base period, which likely leads to a slight overestimate of the meltwater here. The effect is negligible though as the meltwater term is a minor contributor to the overall 20th century sea level rise.

403 1) ANNUAL

404 Table 5 shows the projected changes in temperature and precipitation for the 30-year
405 periods centered around the 2020s, 2050s, and 2080s relative to the baseline period. The values
406 shown are the central range (middle 67%) of the projected model-based changes.

407 Figure 6 expands upon the information presented in Table 5 in three ways. First,
408 inclusion of observed data since 1900 provides context on how the scale of projected changes
409 associated with forcing from greenhouse gases and other radiatively important agents compares
410 to historical variations and trends. Secondly, tabulating high and low projections across all 48
411 simulations provides a broader range of possible outcomes, which some stakeholders requested
412 (New York City Climate Change Adaptation Task Force, 2008-2009). Finally, ensemble
413 averaging of results by emissions scenario as they evolve over time is informative to
414 stakeholders involved in greenhouse gas mitigation (and adaptation), since it reveals the large
415 system inertia: not until the 2030s and 2040s do the B1 scenario projections begin to diverge
416 from A2 and A1B, but thereafter it diverges rapidly. Thus, a delay in greenhouse gas mitigation
417 activities greatly increases the risk of severe long-term climate change consequences, despite
418 apparent similarity in the near-term outlook.

419 While the precise numbers in Table 5 and Figure 6 should not be emphasized due to high
420 uncertainty and the smoothing effects of ensemble averaging, the stakeholder sees that in the
421 New York Metropolitan Region: 1) mean temperatures and sea levels are projected to increase in
422 all simulations this century, at rates exceeding those experienced in the 20th century; 2) while
423 precipitation is projected to increase slightly in most simulations, the multi-year precipitation
424 range experienced in the past century due to climate variability exceeds the 21st century climate

425 change signal[13]; and 3) climate projection uncertainties grow throughout the 21st century, in step
426 with uncertainties regarding future emissions and the climate system response.
427
428 2) SEASONAL
429 Warming in the New York City region is of similar magnitude for all seasons in the
430 GCMs, although seasonal projections are characterized by larger uncertainties than annual
431 projections (Fig. 7a). Since interannual temperature variability is smallest in summer this
432 suggests the summer warming may produce the largest departures from historical experience.
433 Some impacts and vulnerabilities are also amplified by high temperatures. Energy demand in
434 New York City is highly sensitive to temperature during heat waves, due especially to increased
435 reliance on air conditioning. This increased demand can lead to elevated risk of power shortages
436 and failures at a time when vulnerable populations are exposed to high heat stress and air
437 pollution (Kinney et al. 2001; Kalkstein 1995; Hill and Goldberg 2001; Hogrefe et al. 2004).
438 GCMs tend to distribute much of the additional precipitation during the winter months
439 (Fig. 7b), when water supply tends to be relatively high and demand relatively low (NYCDEP
440 2008). During September and October, a time of relatively high drought risk, total precipitation
441 is projected to decrease slightly in many models.
442

[13] The projection lines in Figure 6 depict the 'predictable' anthropogenic forcing component, while capturing some of the uncertainty associated with greenhouse gas concentrations and climate sensitivity at specific points in time. Because decadal variability is unpredictable in the Northeast, it was not included in the time-specific projection portion of the figure. It was however emphasized to stakeholders that while interannual variability appears greatly reduced in the projection portion of the figure, the observed portion (black line) reflects the type of unpredictable variations that have been experienced in the past and will likely exist on top of the mean change signal in the future.

443 *b. Sea Level Rise*

444 Addition of the two regional components leads to higher sea level rise projections for the
445 region than the global average (by ~15 cm for end-of-century projections; Meehl et al. 2007b;
446 Peltier 2001). This is due both to land subsidence and higher sea level rise along the northeast
447 U.S. coast, the latter largely due to geostrophic constraints associated with projected weakening
448 of the Gulf Stream (Yin et al. 2009) in many GCMs (Meehl et al. 2007b).

449 As shown in Table 6, the rapid ice melt scenario projections diverge from the IPCC-
450 based approach as the century progresses. The 2100 value of up to ~2 meters associated with
451 this scenario (not shown) is generally consistent with other recent results that roughly constrain
452 sea level rise globally (see e.g., Pfeffer et al. 2008; Rahmstorf, 2007; Horton et al. 2008; Grinsted
453 2009; Rignot and Cazenave 2009) and regionally (see Yin et al. 2009; Hu et al. 2009) to between
454 ~1m and ~2m. The consistency with other studies supports the usefulness of ~2m as a high end
455 for a risk-averse approach to century-scale infrastructure investments including bridges and
456 tunnels, rail lines, and water infrastructure.

457 At the request of agencies that manage some of these long-term investments, two
458 presentations were given to technical staff specifically describing the rapid ice melt methodology
459 and projections. While these and other stakeholders wanted to know the probability of the rapid
460 ice melt scenario relative to the IPCC-based method, it was emphasized that such probability
461 statements are not possible given current scientific understanding.

462

463 *c. Extreme Events*

464 1) STAKEHOLDER PROJECTIONS BASED ON THE DELTA METHOD

465 Table 7 shows projected changes in the frequency of heat waves, cold events, intense

466 precipitation, and coastal flooding in the New York City region. The baseline average number of
467 extreme events per year is shown, along with the central range (middle 67%) of the projections.
468 Because the distribution of extreme events around the (shifting) mean could also change while
469 mean temperature, precipitation, and sea level rise shift, stakeholders were strongly encouraged
470 to focus only on the direction and relative magnitudes of the extreme event changes in Table 7.

471 The key finding for most stakeholders is the extent to which mean shifts alone can
472 produce dramatic changes in the frequency of extreme events, such as heat events and coastal
473 storm surges. Based on the central range, the number of days per year over 90 ºF is projected to
474 increase by a factor of approximately three by the 2080s. The IPCC-based sea level rise
475 projections alone, without any changes in the historical storm climatology and surge levels, lead
476 to a more than threefold increase in the frequency of the baseline 1-in-10 year coastal flood event
477 by the 2080s.

478 In contrast to relatively homogeneous mean climate changes, it was emphasized to
479 stakeholders that absolute extreme event projections like days below freezing and days with
480 more than one inch of precipitation vary dramatically throughout the metropolitan region, since
481 they depend for example on microclimates associated with the urban heat island and proximity to
482 the coast. Similarly, maps were generated for stakeholders to show that the surge heights for the
483 open estuary at the Battery are higher than corresponding heights in more protected riverine
484 settings.

485 It was emphasized to stakeholders that due to large interannual variability in extremes,
486 even as the climate change signal strengthens, years with relatively few extreme heat events
487 (relative to today's climatology) will occur. For example, Central Park's temperatures in 2004
488 only exceeded 90°F (~32°C) twice. The delta method suggests that not until the middle of this

489 century would such a relatively cool summer (as 2004) feature more days above 90°F (~32°C)
490 than are typically experienced today.

491 High year-to-year extreme event variability may already give some stakeholders a
492 framework for assessing sector-specific climate change impacts; even if climate adaptation
493 strategies for extremes are not already in place, short-term benefits may be evident to planners.
494 For example, Central Park in 2010 experienced temperatures of higher than 90°F (~32°C), on 32
495 different days, which is consistent with projections for a typical year around mid-century. This
496 suggests that some of the infrastructure impacts of extreme heat (such as voltage fluctuations
497 along sagging power lines and increased strain on transportation materials including rails and
498 asphalt; Horton and Rosenzweig 2010) may have been experienced in 2010 to an extent that may
499 become typical by mid-century. However, adaptation strategies designed for an extreme year
500 today (such as a fixed level of mandatory energy use reductions and a fixed level of reductions of
501 train speeds) may be inadequate or unpalatable in the future due to the increase in frequency,
502 duration and intensity of extreme heat (for example) associated with climate change (see e.g.,
503 Meehl et al. 2009; Tebaldi et al. 2006; Meehl and Tebaldi 2004).
504
505 *2) GCM changes in intra-annual distributions*

506 Since high frequency events are not well-simulated in GCMs, the results described here
507 were not included in the New York City adaptation assessment; they are explored here as an
508 exercise, since there is the possibility of distributional changes in the future. The daily
509 distribution of: a) maximum temperatures[14] in summer (JJA), and b) minimum temperatures in

[14] Precipitation was excluded, based on the preliminary analysis of hindcast daily precipitation described in section 3d.

510 winter (DJF) are analyzed in the three GCMs described earlier (CSIRO, GISS and ECHAM5;
511 section 3d), both for the 1980-1999 hindcast and the 2080-2099 A1B experiment.

512 The results indicate that GCM temperature changes in the region in some cases do reflect
513 more than a shifting mean. The intra-annual standard deviation[15] of winter minima decreases in
514 all three GCMs (in two cases by approximately 10 %), while summer standard deviation changes
515 are negligible. One tail of a season's distribution can be more affected than the other; as shown
516 in Fig. 8 for CSIRO, the winter minimum changes are more pronounced on anomalously cold
517 days than anomalously warm days. All 3 GCMs show a larger shift in the coldest 1% of the
518 distribution than the highest 1%. This asymmetry at the 1% tails is most pronounced in CSIRO,
519 where the future coldest 1% event occurs 8 times more often in the baseline, while the baseline
520 warmest 1% event occurs three times more often in the future.
521
522 *d. Comparison of GCM gridbox based-projections to other downscaling methods*
523 The GCM grid box results used for the New York assessment were compared to
524 statistically downscaled results from Bias-Corrected and Spatially-Downscaled (BCSD) Climate
525 Projections at 1/8 degree resolution derived from the World Climate Research Programme's
526 (WCRP's) Coupled Model Intercomparison Project Phase 3 (CMIP3) multi-model dataset. The
527 BCSD projections are available at: http://gdo-dcp.ucllnl.org/downscaled_cmip3_projections/
528 (Maurer, 2007). Results were also compared to simulations from four parings of GCMs and
529 RCMs (Table 8) contributing to the North American Regional Climate Change Assessment
530 Program (NARCCAP; Mearns et al. 2009). Comparison of the three methods is limited to the

[15] As calculated separately for each year and then averaged across the 20 years, to minimize the role of interannual variability.

2050s timeslice under the A2 emissions scenario relative to the 1970-1999 baseline, since NARCCAP projections are not available for other emissions scenarios or time periods. The comparison focuses on projections rather than validation, since the BCSD methodology by definition includes bias correction whereby the baseline GCM outputs are adjusted to match the observed mean and variance. Preliminary analysis of NARCCAP results indicates that these simulations, like GCM projections, require bias correction.

The ensemble mean changes for the GCM gridbox, BCSD, and RCM approaches differ from each other by no more than .3ºC for temperature and 3% for precipitation. The intermodel temperature range is slightly larger for the GCM gridbox approach than BCSD, while the opposite is the case for precipitation. The four RCM simulations perhaps not surprisingly feature a smaller intermodel range than the 16 ensemble members for the GCM gridbox and BCSD approaches.

The number of days above 90 ºF was evaluated as a measure of extremes events. The delta method applied to the GCM gridbox and BCSD[16] produce virtually identical results (increases of approximately 185 and 180 percent respectively in the number of days above 90ºF). When actual daily values from RCMs are used the increase is approximately 170 percent. When the delta method from the RCMs is applied to the observations, the increase is approximately 195 percent.

For mean changes and the daily extreme metric assessed here, BCSD and the four RCMs offer comparable results to the single gridbox GCM approach in the New York Metropolitan Region. Future research will assess how statistical and dynamic downscaling perform in more specialized contexts tailored to unique stakeholder needs that are beyond the scope of New York

[16] At the time of analysis, BCSD is only available at monthly resolution.

553 City initial assessment. For example, reservoir managers concerned with water turbidity might
554 desire information about sequences of days with intense precipitation during particular times of
555 year. Future research will also explore the pros and cons of projections that incorporate highly
556 uncertain modeled changes in interannual variance through time[17].
557

558 # 5. Conclusions and Recommendations for Future Work

559 A framework for climate hazard assessment geared towards adaptation planning and
560 decision support is described. This single GCM gridbox, delta method-based approach, designed
561 for cities and regions smaller than typical GCM gridbox sizes that face resource and time
562 constraints, achieves comparable results in the New York Metropolitan Region to other
563 statistically and dynamically downscaled products. When applied to high frequency historical
564 data, long-term mean monthly climate *changes* (which GCMs are expected to simulate more
565 realistically for point locations than other features such as *actual* long-term mean climate or high
566 frequency statistics) yield dramatic changes in the frequency of stakeholder-relevant climate
567 hazards such as coastal flooding and heat events. While the precise projections should not be
568 emphasized given the uncertainties, they are of sufficient magnitude relative to the historical
569 hazard profile to justify development and initial prioritization of adaptation strategies. This
570 process is now well underway in the New York Metropolitan Region.
571 When climate model results for the New York Metropolitan Region are used only for the
572 calculation of monthly climate change factors based on the differences and ratios between 30-

[17] Preliminary analysis reveals that over the New York Metropolitan Region gridbox a slight majority of the GCMs show increasing interannual variance of monthly T and P, while a large majority of the BCSD and NARCCAP RCM projections do.

573 year future timeslices and a 30-year baseline period, three generalized findings follow. First,
574 using multiple ensemble members from the same GCM provides little additional information,
575 since the 30-year average intramodel ranges are smaller than the comparable inter-model range.
576 Second, the spatial pattern of climate change factors in many regions (including New York City)
577 is sufficiently homogeneous --- relative to the intermodel range --- to justify use of climate
578 change factors from a single overlying GCM gridbox. Finally, for these metrics, newer
579 statistically (BCSD) and dynamically (four NARCCAP RCMs) downscaled products provide
580 comparable results to the GCM single gridbox output used by the NPCC.

581 The checklist in Table 2 provides a series of questions to help inform the selection of the
582 most appropriate climate hazard assessment and projection methods. For example, the delta
583 method is more justified when: 1) robust, long-term historical statistics are available, and 2)
584 evidence of how modes of interannual and interdecadal variability and their local teleconnections
585 will change with climate change is inconclusive. Both these criteria are met in the New York
586 City Metropolitan Region. In contrast, more complex applications (than the delta method) of
587 statistically and dynamically downscaled products especially may be more appropriate when
588 spatially continuous projections are needed over larger regions with complex topography. For
589 example, where a large mountain range is associated with a strong precipitation gradient at sub-
590 GCM gridbox scales, percentage changes in precipitation might also be expected to be more
591 spatially heterogeneous than in the New York Metropolitan Region.

592 Extreme event projections, so frequently sought by stakeholders for impact analysis, will
593 likely improve as statistical and dynamical downscaling evolve. RCMs especially hold promise
594 for assessing how 'slow' variations associated with climate change and variability will affect the
595 future distribution of 'fast' extremes like subdaily rainfall events. Nevertheless, translating RCM

596 simulations into stakeholder-relevant projections requires many of the same adjustments and
597 caveats described here for GCMs (such as bias correction). Statistical downscaling techniques
598 also hold promise as well for the simulation of extremes (non-stationarity not withstanding), to
599 the extent that predictor variables are well simulated by GCMs and linkable to policy relevant
600 local climate variables. Projections of extremes will also benefit from improved estimates of
601 historical extremes (such as the 1-in-100 year drought and coastal flood) as long-term tree ring
602 and sediment records (for example) are increasingly utilized.

603 There is also a need for improved simulation of climate variability at interannual to
604 decadal scales, as this is the time horizon for investment decisions and infrastructure lifetime in
605 many sectors, including telecommunications (NPCC, 2010). The limits to such predictability are
606 beginning to be explored in Coupled Model Intercomparison Project (CMIP5) experiments
607 initialized with observed ocean data, but this is a long-term research issue.

608 An absence of local climate projections need not preclude consideration of adaptation.
609 For many locales, climate changes in other regions may rival the importance of local changes by
610 influencing migration, trade, and ecosystem and human health, for example. Furthermore, some
611 hazards such as drought are often regional phenomena, with multi-state policy implications (such
612 as water-sharing agreements). Finally, since climate vulnerability depends on many non-climatic
613 factors (such as poverty), some adaptation strategies (such as poverty-reduction measures) can be
614 commenced in advance of climate projections.

615 Monitoring of climate indicators should be encouraged since it reduces uncertainties and
616 leads to refined projections. Locally, sustained high temporal resolution observation networks
617 can provide needed microclimatic information, including spatial and temporal variation in
618 extreme events such as convective rainfall and storm surge propagation. At the global scale,

monitoring of polar ice sheets and global sea level will improve understanding of sea level rise. Periodic assessments of evolving climate, impacts and adaptation science will support flexible/recursive adaptation strategies that minimize the impact of climate hazards while maximizing societal benefits.

Acknowledgments

This work was supported by the Rockefeller Foundation. We acknowledge the modeling groups, the Program for Climate Model Diagnosis and Intercomparison (PCMDI) and the WCRP for the CMIP3 multi-model dataset, supported by the Office of Science, U.S. Department of Energy. We thank Jonathan Gregory for additional GCM output not available from the WCRP dataset. We also thank Adam Freed and Aaron Koch from the Mayor's Office of Long Term Planning and Sustainability, and Malcolm Bowman from the NPCC, for comments on prior work that helped inform this paper. Finally with thank the anonymous reviewers of this manuscript.

REFERENCES

Amato, A. D., M. Ruth, P. Kirshen, and J. Horwitz, 2005: Regional energy demand responses to climate change: Methodology and application to the Commonwealth of Massachusetts. *Climatic Change*, **71,** 175-201.

Arnell, N. W., 1996: *Global Warming, River Flows, and Water Resources.* Wiley, 234 pp.

ASCE, 2009: 2009 Report Card for American Infrastructure American Society of Civil Engineers 153 pp.

Bardossy, A., and E. Plate, 1992: Space-time model for daily rainfall using atmospheric circulation patterns. *Water Resources Research*, **28,** 1247 - 1259.

Bindoff, N. L., and Coauthors, 2007: Observations: Oceanic Climate Change and Sea Level. *Climate Change 2007: The Physical Science Basis. Contribution of Working Group I to the Fourth Assessment Report of the Intergovernmental Panel on Climate Change.*, S. Solomon, and Coauthors, Eds., Cambridge University Press, 386 - 432.

Bradbury, J. A., B. D. Keim, and C. P. Wake, 2002: U.S. East Coast trough indices at 500 hPa and New England winter climate variability. *Journal of Climate*, **15,** 3509-3517.

Brekke, L. D., M. D. Dettinger, E. P. Maurer, and M. Anderson, 2008: Significance of model credibility in estimating climate projection distributions for regional hydroclimatological risk assessments. *Climatic Change*, **89,** 371 - 394.

Caya, D., and R. Laprise, 1999: A semi-implicit semi-Lagrangian regional climate model: The Canadian RCM, *Mon. Weather Rev.*, **127**, 341-362.

Chen, J. L., C. R. Wilson, D. Blakenship, and B. D. Tapley, 2009: Accelerated Antarctic ice loss from satellite gravity measurements. *Nature Geoscience*, **2,** 859 - 862.

654 Christensen, J. H., and Coauthors, 2007: Regional Climate Projections. *Climate Change 2007:*
655 *The Physical Science Basis. Contribution of Working Group I to the Fourth Assessment*
656 *Report of the Intergovernmental Panel on Climate Change*, S. Solomon, and Coauthors,
657 Eds., Cambridge University Press, 849 - 940.
658 Collins, W. D., and Coauthors, 2006: The Community Climate System Model CCSM3. *Journal*
659 *of Climate*, **19,** 2122 - 2143.
660 Cubasch, U., and Coauthors, 2001: Projections of future climate change. *Climate Change 2001:*
661 *The Scientific Basis: Contribution of Working Group I to the Third Assessment Report of*
662 *the Intergovernmental Panel on Climate Change*, J. T. Houghton, Ed., Cambridge
663 University Press, 525 - 582.
664 Delworth, T. L., and Coauthors, 2006: GFDL's CM2 global coupled cliamte models - Part1:
665 Formulation and simulation characteristics. *Journal of Climate*, **19,** 643 - 674.
666 Easterling, D. R., T. R. Karl, J. H. Lawrimore, and S. A. Del Greco, 1999: United States
667 Historical Climatology Network Daily Temperature and Precipitation Data (1891 - 1997),
668 ORNL/CDIAC-118, NDP-070, Carbon Dioxide Information Analysis Center, Oak Ridge
669 National Laboratory, Oak Ridge, TN.
670 Emori, S., and S. J. Brown, 2005: Dynamic and thermodynamic changes in mean and extreme
671 precipitation under changed climate. *Geophysical Research Letters*, **32,**
672 L17706,doi:17710.11029/12005GL023272.
673 Evan, A. T., J. P. Dunion, J. A. Foley, A. K. Heidinger, and C. S. Velden, 2006: New evidence
674 for a relationship between Atlantic tropical cyclone activity and African dust outbreaks.
675 *Geophysical Research Letters*, **33,** L19813,doi:19810.11029/12006GL026408.

676 Fairbanks, R. G., 1989: 17,000-year glacio-eustatic sea level record: influence of glacial melting
677 rates on the Younger Dryas event and deep-ocean circulation. *Nature*, **342,** 637 - 642.
678 Flato, G. M., 2005: The Third Generation Coupled Global Climate Model (CGCM3) (and
679 included links to the description of the AGCM3 atmospheric model).
680 http://www.cccma.bc.ec.gc.ca/models/cgcm3.shtml.
681 Furevik, T., and Coauthors, 2003: Description and evaluation of the Bergen climate model:
682 ARPEGE coupled with MICOM. *Climate Dynamics*, **21,** 27 - 51.
683 Gaffin, S. R., and Coauthors, 2008: Variations in New York City's urban heat island strength
684 over time and space. *Theoretical and Applied Climatology* **94,** 1-11.
685 Giorgi, F., C. Jones, and G.R. Asrar, 2009: Addressing Climate Information Needs at the
686 Regional Level: The CORDEX Framework. *WMO Bulletin,* **58(3)**, 175-183
687 Giorgi, F., and L. O. Mearns, 2002: Calculation of Average, Uncertainty Range, and Reliability
688 of Regional Climate Changes from AOGCM Simulations via the "Reliability Ensemble
689 Averaging" (REA) Method. Journal of Climate, 15, 1141-1158.
690 Gleick, P. H., 1986: Methods for evaluating the regional hydrologic effects of global cliamte
691 changes. *Journal of Hydrology*, **88,** 97 - 116.
692 Gordon, H. B., and Coauthors, 2002: The CSIRO Mk3 Climate System Model. CSIRO
693 Atmospheric Research Technical Paper No. 60, Commonwealth Scientific and Industrial
694 Research Organisation Atmospheric Research, Aspendale, Victoria, Australia., 130 pp.
695 Gornitz, V., 2001: Sea-level rise and coasts. *Climate change a global city: The potential*
696 *consequences of climate variability and change, Metro East Coast*, C. Rosenzweig, and
697 W. D. Solecki, Eds., Report for the U.S. Global Change Research Program, Columbia
698 Earth Institute, 121-148.

699 Greene, A. M., L. Goddard, and U. Lall, 2006: Probabilistic multimodel regional temperature
700 change projections. *Journal of Climate*, **19,** 97 - 116.
701 Grinsted, A., J. C. Moore, and S. Jevrejeva, 2009: Reconstructing sea level from paleo and
702 projected temperatures 2000 to 2100 A.D. *Climate Dynamics***,** doi:10.1007/s00382-
703 00008-00507-00382.
704 Grotch, S. L., and M. C. MacCracken, 1991: The use of general circulation models to predict
705 regional climatic change. *Journal of Climate*, **4,** 286 - 303.
706 Hansen, J., M. Sato, P. Kharecha, G. Russell, D. W. Lea, and M. Siddall, 2007: Climate changes
707 and trace gases. *Philosophical Transactions of The Royal Society*, **365,** 1925 - 1954.
708 Hayhoe, K., and Coauthors, 2007: Past and future changes in climate and hydrological indicators
709 in the US Northeast. *Climate Dynamics* **28,** 381-407.
710 Hegerl, G. C., and Coauthors, 2007: Understanding and Attributing Climate Change *Climate*
711 *Change 2007: The Physical Science Basis. Contribution of Working Group I to the*
712 *Fourth Assessment Report of the Intergovernmental Panel on Climate Change*, S.
713 Solomon, and Coauthors, Eds., Cambridge University Press, 664 - 745.
714 Hill, D., and R. Goldberg, 2001: Energy Demand. *Climate change a global city: The potential*
715 *consequences of climate variability and change, Metro East Coast*, C. Rosenzweig, and
716 W. D. Solecki, Eds., Report for the U.S. Global Change Research Program, Columbia
717 Earth Institute, 121-148.
718 Hogrefe, C., and Coauthors, 2004: Health impacts from cliamte-change induced changes in
719 ozone level in 85 United States cities. *Epidemiology*, **15,** 94-95.

720 Horton, R., and C. Rosenzweig, 2010: Climate Risk Information. *Climate change adaptation in*
721 *New York City: Building a Risk Management Response*, C. Rosenzweig, and W. Solecki,
722 Eds., New York Academy of Sciences.
723 Horton, R., C. Herweijer, C. Rosenzweig, J. P. Liu, V. Gornitz, and A. C. Ruane, 2008: Sea level
724 rise projections for current generation CGCMs based on the semi-empirical method.
725 *Geophysical Research Letters*, **35,** L02715,doi:02710.01029/02007GL032486.
726 Hu, A., G. A. Meehl, W. Han, and J. Yin, 2009: Transient response of the MOC and climate to
727 potential melting of the Greenland Ice Sheet in the 21st Century. *Geophysical Research*
728 *Letters*, **36,** L10707,doi:10710.11029/12009GL037998.
729 IPCC, 2007: *Climate Change 2007: The Physical Science Basis*. Contribution of Working Group
730 I to the Fourth Assessment Report of the Intergovernmental Panel on Climate Change,
731 996 pp.
732 Jones, R.G., and Coauthors, 2004: Generating high-resolution climate change scenarios using
733 PRECIS. Exter, UK, Available from MET Office Hadley Centre.
734 Johns, T. C., and Coauthors, 2006: The new Hadley Centre climate model HadGEM1:
735 Evaluation of coupled simulations. *Journal of Climate*, **19,** 1327 - 1353.
736 Jungclaus, J. H., and Coauthors, 2006: Ocean circulation and tropical variability in the AOGCM
737 ECHAM5/MPI-OM. *Journal of Climate*, **19,** 3952-3972.
738 K-1 Model Developers, 2004: K-1 Technical Report. Center for Climate System Research,
739 University of Tokyo, Tokyo, Japan, 34 pp.
740 Kalkstein, L., 1995: Reported in D. MacKenzie, Deadly face of summer in the city. *New*
741 *Scientist*, 4.

742 Kanamitsu, M., W. Ebisuzaki, J. Woollen, S.-K. Yang, J. J. Hnilo, M. Fiorino, and G. L. Potter,
743 2002: NCEP/DOE AMIP-II Reanalysis (R-2). *Bulletin of the American Meteorological*
744 *Society*, **83,** 1631 - 1643.
745 Karl, T. R., C. N. Williams, F. T. Quinlan, and T. A. Boden, 1990: United States Historical
746 Climatology Network (HCN) Serial Temperature and Precipitation Data, Publ. 304,
747 Environmental Science Division, Carbon Dioxide Information and Analysis Center, Oak
748 Ridge National Laboratory, Oak Ridge, TN, 389 pp.
749 Kinney, P. L., D. Shindell, E. Chae, and B. Winston, 2001: Public health. *Climate change a*
750 *global city: The potential consequences of climate variability and change, Metro East*
751 *Coast*, C. Rosenzweig, and W. D. Solecki, Eds., Report for the U.S. Global Change
752 Research Program, Columbia Earth Institute, 103-120.
753 Le Quere, C., and Coauthors 2009: Trends in the sources and sinks of carbon dioxide. *Nature*
754 *Geoscience*, **2,** 831-836.
755 Marti, O., and Coauthors, 2005: The New IPSL Climate System Model: IPSL-CM4. Note du
756 Pôle de Modélisation No. 26, Institut Pierre Simon Laplace des Sciences de
757 l'Environnement Global, Paris.
758 Maurer, E. P., L. Brekke, T. Pruitt, and P. B. Duffy, 2007: Fine-resolution climate projections
759 enhance regional climate change impact studies. *Eos Trans. AGU*, **88,** 504.
760 Mearns, L. O., W. Gutowski, R. Jones, R. Leung, S. McGinnis, A. Nunes, and Y. Qian, 2009: A
761 regional climate change assessment program for North America. *Eos Trans. AGU*, **90,**
762 311.
763 Meehl, G. A., and C. Tebaldi, 2004: More intense, more frequent, and longer lasting heat waves
764 in the 21st century. *Science*, **305,** 994 - 997.

765 Meehl, G. A., J. M. Arblaster, and C. Tebaldi, 2005: Understanding future patterns of increased
766 precipiation intensity in climate model simulations. *Geophysical Research Letters*, **32,**
767 L18719,doi:18710.11029/12005GL023680.
768 Meehl, G. A., and Coauthors, 2007a: The WCRP CMIP3 multi-model dataset: A new era in
769 climate change research. *Bulletin of the American Meteorological Society*, **88,** 1383-
770 1394.
771 ——, 2007b: Global Climate Projections. *Climate Change 2007: The Physical Science*
772 *Basis. Contribution of Working Group I to the Fourth Assessment Report of the*
773 *Intergovernmental Panel on Climate Change*, S. Solomon, and Coauthors, Eds.,
774 Cambridge University Press, 747 - 845.
775 Meehl, G. A., C. Tebaldi, G. Walton, D. Easterling, and L. McDaniel, 2009: Relative increase of
776 record high maximum temperatures compared to record low minimum temperatures in
777 the U.S. *Geophysical Research Letters*, **36,** 23,doi:10.1029/2009GL040736.
778 Min, S.-K., S. Legutke, A. Hense, and W.-T. Kwon, 2005: Climatology and internal variability
779 in a 1000-year control simulation with the coupled climate model ECHO-G—I. Near-
780 surface temperature, precipitation and mean sea level pressure. *Tellus*, **57A,** 605 - 621.
781 Mitrovica, J. X., N. Gomez, and P. U. Clark, 2009: The sea-level fingerprint of West Antarctic
782 collapse. *Science*, **323,** 753.
783 Mitrovica, J. X., M. Tamisiea, J. L. Davis, and G. A. Milne, 2001: Recent mass balance of polar
784 ice sheets inferred from patters of global sea-level change. *Nature*, **409,** 1026 - 1029.
785 Mote, P., A. Petersen, S. Reeder, H. Shipman, and W. Binder, 2008: Sea Level Rise in the
786 Coastal Waters of Washington State, University of Washington Climate Impacts Group
787 and the Washington Department of Ecology, 11 pp.

MTA, 2007: Metropolitan Transportation Authority August 8, 2007 Storm Report.

Nakicenovic, N., and Coauthors, 2000: Special Report on Emissions Scenarios: A Special Report of Working Group III of the Intergovernmental Panel on Climate Change, 599 pp.

Namias, J., 1966: Nature and possible causes of the Northeastern United States drought during 1962065. *Monthly Weather Review*, **94,** 543-554.

NRC, 2009: *Informing Decisions in a Changing Climate. Panel on Strategies and Methods for Climate-Related Decision Support.* Washington, DC: The National Academies Press.

NRC, 2010a: America's Climate Choices: Panel on Advancing the Science of Climate Change; *Advancing the Science of Climate Change.* Washington D.C.: The National Academies Press.

——, 2010b: America's Climate Choices: Panel on Adapting to the Impacts of Climate Change; *Adapting to the Impacts of Climate Change.* Washington D.C.: The National Academies Press.

New York City Climate Change Adaptation Task Force and Working Group Meetings, Mayor's Office of Long Term Planning and Sustainability, New York, New York, 2008 - 2009.

New York City Office of the Mayor. 17 February 2009. Mayor Bloomberg Releases New York City Panel on Climate Change Report that Predicts Higher Temperatures and Rising Sea Levels for New York City.

Nicholls, R. J., S. Hanson, and C. Herweiger, 2008: Ranking Port Cities with High Exposure and Vulnerability to Climate Extremes: Exposure Estimates, OECD Environment Working Papers, No.1, OECD Publishing

NPCC. 2010. Climate Change Adaptation in New York City: Building a Risk Management Response. C. Rosenzweig and W. Solecki, Eds. Prepared for use by the New York City Climate Change Adaptation Task Force. Annals of the New York Academy of Science, 2010. New York, NY.

813 NYCDEP, 2008: Report 1: Assessment and Action Plan - A Report Based on the Ongoing Work
814 of the DEP Climate Change Task Force.
815 Pal, J.S., and Coauthors, 2007. Regional climate modeling for the developing world: The ICTP
816 RegCM3 and RegCNET. *Bull. Amer. Meteor. Soc.*, **88**, 1395 - 1409.
817 Peltier, W. R., 2001: Global glacial isostatic adjustment and modern instrumental records of
818 relative sea level history. *Sea Level Rise: History and Consequences*, B. C. Douglas, M.
819 S. Kearney, and S. P. Leatherman, Eds., Academic Press, 65 - 95.
820 Peltier, W. R., and R. G. Fairbanks, 2006: Global glacial ice volumen and last glacial maximum
821 duration from an extended Barbados sea level record. *Quaternary Science Reviews*, **25,**
822 3322 - 3337.
823 Pfeffer, W. T., J. T. Harper, and S. O'Neel, 2008: Kinematic constraints on glacier contributions
824 to 21st-century sea-level rise. *Science*, **321,** 1340 - 1343.
825 PlaNYC, 2008: Sustainable stormwater management plan 2008. Mayor's Office of Long-Term
826 Planning and Sustainability, 86 pp.
827 Rahmstorf, S., 2007: A semi-empirical approach to projections future sea level rise. *Science*,
828 **315,** 368 - 370.
829 Randall, D. A., and Coauthors, 2007: Climate Models and Their Evaluation. *Climate Change*
830 *2007: The Physical Science Basis. Contribution of Working Group I to the Fourth*
831 *Assessment Report of the Intergovernmental Panel on Climate Change*, S. Solomon, and
832 Coauthors, Eds., Cambridge University Press, 590 - 662.
833 Rignot, E., and A. Cazenave, 2009: Ice Sheets and Sea Level Rise Feedbacks. *Arctic Climate*
834 *Feedbacks: Global Implications*, M. Sommerkorn, and S. J. Hassol, Eds., WWF
835 International Arctic Programme.

836 Rind, D., M. Chin, G. Feingold, D. Streets, R. A. Kahn, S. E. Schwartz, and H. Yu, 2009:
837 Modeling the effects of aerosols on climate. *Aerosol Properties and Their Impacts on*
838 *Climate, U.S. Climate Change Science Program Synthesis and Assessment Product 2.3*,
839 M. Chin, R. A. Kahn, and S. E. Schwartz, Eds., National Aeronautics and Space
840 Administration, 64 - 97.
841 Rohling, E. J., K. Grant, C. H. Hemleben, M. Siddall, B. A. A. Hoogakker, M. Bolshaw, and M.
842 Kucery, 2008: High rates of sea-level rise during the last interglacial period. *Nature*
843 *Geoscience*, **1,** 38 - 42.
844 MEC, 2001. Climate change and a Global City: The Potential Consequences of Climate
845 Variability and Change, Metro East Coast. C. Rosenzweig and W.D. Solecki, Eds. Report
846 for the US Global Change Research Program. Columbia Earth Institute.
847 Rosenzweig, C., W. D. Solecki, L. Parshall, and S. Hodges, Eds., 2006: *Mitigating New York*
848 *city's heat island with urban forestry, living roofs, and light surfaces, New York City*
849 *Regional Heat Island Initiative, Final Report 06-06, New York State Energy Research*
850 *and Development Authority*. 133 pp.
851 Rosenzweig, C., D. C. Major, K. Demong, C. Stanton, R. Horton, and M. Stults, 2007: Managing
852 climate change risks in New York City's water system: Assessment and adaptation
853 planning. *Mitigation and Adaptation Strategies for Global Change*, **12,** 1391 - 1409.
854 Schmidt, G. A., and Coauthors, 2006: Present day atmospheric simulations using GISS ModelE:
855 Comparison to in-situ, satellite and reanalysis data. *Journal of Climate*, **19,** 153 - 192.
856 Shepherd, A., and D. Wingham, 2007: Recent sea-level contributions of the Antarctic and
857 Greenland ice sheets. *Science*, **315,** 1529 - 1532.

858 Solecki, W. D., L. Patrick, and M. Brady, 2010: Climate Protection Levels: Incorporating
859 climate change into design and performance standards. *Climate change adaptation in*
860 *New York City: Building a Risk Management Response*, C. Rosenzweig, and W. D.
861 Solecki, Eds., New York Academy of Sciences.
862 Smith, R. L., C. Tebaldi, D. Nychka, and L. O. Mearns, 2009: Bayesian Modeling of Uncertainty
863 in Ensembles of Climate Models. *Journal of the American Statistical Association*, **104,**
864 97 - 116.
865 Sussman, E., and D.C. Major, 2010: Law and regulation. *Climate change adaptation in New*
866 *York City: Building a Risk Management Response*, C. Rosenzweig, and W. Solecki, Eds.,
867 New York Academy of Sciences.
868 Tebaldi, C., R. L. Smith, D. Nychka, and L. O. Mearns, 2005: Quantifying uncertainty in
869 projections of regional climate change: a Bayesian approach to the analysis of
870 multimodel ensembles. *Journal of Climate*, **18,** 1524.
871 Tebaldi, C., K. Hayhoe, J. M. Arblaster, and G. A. Meehl, 2006: Going to the extremes: an
872 intercomparison of model-simulated historical and future changes in extreme events.
873 *Climatic Change*, **79,** 185 - 211.
874 Terray, L. S., S. Valcke, and A. Piacentini, 1998: OASIS 2.2 Guide and Reference Manual.
875 Technical Report TR/CMGC/98-05, Centre Europeen de Recherche et de Formation
876 Avancée en Calcul Scientifique, Toulouse, France.
877 Volodin, E. M., and N. A. Diansky, 2004: El-Niño reproduction in a coupled general circulation
878 model of atmosphere and ocean. . *Russian Meteorology and Hydrology*, **12,** 5 - 14.
879 Washington, W. M., and Coauthors, 2000: Parallel Climate Model (PCM) control and transient
880 simulations. *Climate Dynamics*, **16,** 755 - 774.

881 Weiss, J., J. Overpeck, and B. Strauss, 2011: Implications of recent sea level rise science for
882 low-elevation areas in coastal cities of the conterminous U.S.A. Climatic Change, 1-11.
883 Weiss, J., J. Overpeck, and B. Strauss, 2011: [Supplemental Material] Implications of recent sea
884 level rise science for low-elevation areas in coastal cities of the conterminous U.S.A.
885 Climatic Change, 1-11.
886 Wigley, T. M., P. D. Jones, K. Briffa, and G. Smith, 1990: Obtaining sub-grid information from
887 course resolution general circulation model output. *Journal of Geophysical Research*, **95,**
888 1943 - 1953.
889 Wilby, R. L., T. M. L. Wigley, D. J. Conway, P. D. Jones, B. C. Hewitson, J. Main, and D. S.
890 Wilks, 1998: Statistical downscaling of general circulation model output: a comparison of
891 methods. *Water Resources Research*, **34,** 2995 - 3008.
892 Wilby, R. L., C. W. Dawson, and E. M. Barrow, 2002: SDSM - A decision support tool for the
893 assessment of regional climate change impacts. *Environmental Modeling and Software*,
894 **17,** 145 - 157.
895 Wilby, R. L., S. Charles, E. Zorita, B. Timbal, P. Whetton, and L. Mearns, 2004: Guidelines for
896 use of climate scenarios developed from statistical downscaling methods. IPCC
897 Supporting Material, available from the DDC of IPPC TGCIA, 27 pp.
898 Williams, C. N., M. J. Menne, R. S. Vose, and D. R. Easterling, 2005: United States Historical
899 Climatology Network Monthly Temperature and Precipiation Data, ORNL/CDIAC-118,
900 NDP-019, Carbon Dioxide Information Analysis Center, Oak Ridge National Laboratory,
901 US Department of Energy, Oak Ridge, TN.
902 WMO, 1989: Calculation of Monthly and Annual 30-Year Standard Normals. *WCDP-*
903 *No.10,WMO-TD/No.341*, World Meteorological Organization.

Wood, A. W., L. R. Leung, V. Sridhar, and D. P. Lettenmaier, 2004: Hydrologic implications of dynamical and statistical approaches to downscaling climate model outputs. *Climatic Change*, **62,** 189 - 216.

Yin, J., M. E. Schlesinger, and R. J. Stouffer, 2009: Model projections of rapid sea-level rise on the Northeast coast of the United States. *Nature Geoscience*, **15,** 1-5.

Yukimoto, S., and A. Noda, 2003: Improvements of the Meteorological Research Institute Global Ocean-Atmosphere Coupled GCM (MRI-GCM2) and its Climate Sensitivity. CGER's Supercomputing Activity Report, National Institute for Environmental Studies, Ibaraki, Japan.

FIGURE CAPTIONS

Figure 1: Satellite map of the New York Metropolitan Region. Shown on the map are the Central Park weather station (circle) and The Battery tide gauge (triangle). Source: ESRI World Imagery.

Figure 2: a) Temperature change (°C) and b) precipitation change (%) for the 2080s timeslice relative to the 1970-1999 model baseline, A1B emissions scenario and 16 GCM ensemble mean.

Figure 3: a) Mean annual temperature for the New York City region, (ºC), 1970-1999 in each of the 16 GCMs, GCM ensemble, Central Park station data and Reanalysis (see methods section for more information). Also shown as hash marks is the interannual standard deviation about the mean for each of the 19 products. b) monthly mean temperature for the New York City region, (ºC), 1970-1999. The two observed products, the GCM ensemble average, and four points in the GCM distribution (lowest, 17th percentile, 83rd percentile, and highest) are shown. c) Mean annual precipitation for the New York City region, (cm), 1970-1999 in each of the 16 GCMs, GCM ensemble, and Central Park observations. Also shown as hash marks is the interannual standard deviation about the mean for each of the 18 products. d) monthly mean precipitation for the New York City region, (cm), 1970-1999. Central park observations, the GCM ensemble average, and four points in the GCM distribution (lowest, 17th percentile, 83rd percentile, and highest) are shown.

Figure 4: Daily distribution (number of days per year) of: a) all-year mean, b) summer (June-August) maximum, and c) winter (December-February) minimum temperature anomalies (ºC),

938 1980-1999 for Central Park observations (black line) and three GCMs (CSIRO, GISS, and MPI
939 ECHAM5).
940
941 Figure 5: Daily distribution (number of days per year) of precipitation (mm), 1980-1999 for
942 Central Park observations (black line) and three GCMs (CSIRO, GISS, and MPI ECHAM5). The
943 first bin, containing less than 10 mm, is not shown.
944
945 Figure 6: Combined observed (black line) and projected: a) temperature (ºC) and b) annual
946 precipitation (mm). Projected model changes through time are applied to the observed historical
947 data. The three thick lines (red, green, and blue) show the ensemble average for each emissions
948 scenario across the 16 GCMs. Shading shows the central 67 % range across the 16 GCMs and 3
949 emissions scenarios. The bottom and top lines, respectively, show each year's minimum and
950 maximum projections across the suite of simulations. A ten-year filter has been applied to the
951 observed data and model output. The dotted area between 2003 and 2015 represents the period
952 that is not covered due to the smoothing procedure.
953
954 Figure 7: Seasonal a) temperature change (ºC) and b) precipitation change (%) projections,
955 relative to the 1970-1999 model baseline, based on 16 GCMs and 3 emissions scenarios. The
956 maximum and minimum are shown as black horizontal lines; the central 67% of values are
957 boxed, and the median is the thick line inside the boxes.
958
959 Figure 8: Daily distribution (number of days per year) of winter (December-February) minimum
960 temperature anomalies (ºC), for the New York Metropolitan Region in the CSIRO GCM. Black

961 line, 1980-1999 hindcast; dotted line, 2080-2099 A1B scenario.

962 TABLE 1. Acronym, host center, atmosphere and ocean grid box resolution, and reference for the 16 GCMs used in the analysis.

Model Acronym	Institution	Atmospheric Resolution (Lat x Lon)	Oceanic Resolution (Lat x Lon)	References
BCCR	Bjerknes Center for Climate Research, Norway	1.9 x 1.9	0.5 to 1.5 x 1.5	Furevik et al., 2003
CCSM	National Center for Atmospheric Research, USA	1.4 x 1.4	0.3 to 1.0 x 1.0	Collins et al., 2006
CGCM	Canadian Center for Climate Modeling and Analysis, Canada	2.8 x 2.8	1.9 x 1.9	Flato 2005
CNRM	National Weather Research Center, METEO-FRANCE, France	2.8 x 2.8	0.5 to 2.0 x 2.0	Terray et al., 1998
CSIRO	CSIRO Atmospheric Research, Australia	1.9 x 1.9	0.8 x 1.9	Gordon et al., 2002
ECHAM5	Max Planck Institute for Meteorology, Germany	1.9 x 1.9	1.5 x 1.5	Jungclaus et al., 2005
ECHO-G	Meteorological Institute of the University of Bonn, Germany	3.75 x 3.75	0.5 to 2.8 x 2.8	Min et al., 2005
GFDL-CM2.0	Geophysical Fluid Dynamics Laboratory, USA	2.0 x 2.5	0.3 to 1.0 x 1.0	Delworth et al., 2006
GFDL-CM2.1	Geophysical Fluid Dynamics Laboratory, USA	2.0 x 2.5	0.3 to 1.0 x 1.0	Delworth et al., 2006

GISS	NASA Goddard Institute for Space Studies	4.0 x 5.0	4.0 x 5.0	Schmidt et al., 2006
INMCM	Institute for Numerical Mathematics, Russia	4.0 x 5.0	2.0 x 2.5	Volodin and Diansky, 2004
IPSL	Pierre Simon Laplace Institute, France	2.5 x 3.75	2.0 x 2.0	Marti, 2005
MIROC	Frontier Research Center for Global Change, Japan	2.8 x 2.8	0.5 to 1.4 x 1.4	K-1 Developers, 2004
MRI	Meteorological Research Institute, Japan	2.8 x 2.8	0.5 to 2.0 x 2.5	Yuikimoto and Noda, 2003
PCM	National Center for Atmospheric Research, USA	2.8 x 2.8	0.5 to 0.7 x 1.1	Washington et al., 2000
UKMO-HadCM3	Hadley Center for Climate Prediction, Met Office, UK	2.5 x 3.75	1.25 x 1.25	Johns et al., 2006

963

964 TABLE 2. Checklist of questions to inform selection of climate hazard assessment and projection methods

Question	Possible implication for choice of method, plus NYC context
1. Are high quality historical data available for a long time period?	When little high-quality historical climate data are available, options for projections are extremely limited. Records of at least several decades are needed to sample the range of natural variability. As RCMs continue to improve, use of raw outputs from RCMs may increasingly be used in such regions, since bias correction and statistical approaches are not feasible without historical climate data. This was not an issue in data-rich NYC.
2. Are projections needed for the entire 21st century?	If yes, this may preclude RCMs due to computational expense. This was an important consideration for NYC, since some sectors such as telecommunications were focused on the 2020s timeslice, while others such as Port Authority of New York and New Jersey manage infrastructure expected to last until 2100.
3. Are multiple emissions scenarios needed, for example to emphasize how mitigation can compliment adaptation?	If yes, RCMs may not be the best approach, since computational expense generally precludes the use of more than 1-2 scenarios.

	This was an important consideration in New York City, since the adaptation effort was part of a broader sustainability effort (PlaNYC) that embraced greenhouse gas mitigation.
4. Are a large group of GCMs and initializations required, in order to sample a broad range of global climate sensitivities and estimates of within-GCM variability, respectively?	If yes, RCMs may not be the best approach, since computational expense generally precludes the use of more than a few GCMs or GCM initializations per RCM. New York City stakeholders expressed interest in the full range of GCM sensitivities.
5. What climate variables are needed, and are they available at the necessary spatial and temporal resolution within public climate model archives?	In NYC, relatively few variables were needed and subdaily information was not required. Additional variable needs at subdaily resolution might argue for the use of RCM archives such as NARCCAP as they continue to be populated, instead of archives such as the first generation of BCSD (monthly temperature and precipitation only). While use of public climate model archives minimizes cost and time, even archived outputs generally require at least some bias and/or scale correction and post-processing for stakeholder applicability.

6. What level of resources are available, and in what time frame is the information needed?	Region and question specific tailored downscaling efforts, as opposed to use of archived downscaled products, may not be possible when resources and time are limited. While NYC had substantial resources available, the short time frame (~8 months) precluded developing new tailored downscaling.
7. Are projections needed for a single in-depth sectoral application and variable in one municipality, or does a large multisectoral and pan-regional group of stakeholders need a coordinated set of scenarios covering a series of standard variables?	In tailored statistical downscaling the method is optimized to the particular location and/or variable. When many variables and a larger region are included, no single optimization method will generally be best for all variables and locations, potentially leading to inconsistencies in either methods or projections across variables and locations. In NYC, the initial emphasis was on generating a common denominator of consistent scenarios based on consistent methods (the delta method) to facilitate coordination across 40 stakeholder entities.
8. Are high-frequency climate inputs that are continuous in time and	If an impacts model is to be run with climate outputs, the range of

space required, such as for input into an impacts model? (e.g., a hydrological model to assess turbidity)	climate and impact results (rather than just the 'delta' mean) will likely be of interest, which may argue for a downscaling technique that allows variance to change, such as BCSD. Statistical downscaling techniques that include weather generators (such as SDSM) may be desirable to create a long record at the needed resolution that includes a range of extreme outcomes for planning purposes. The larger the continuous geographic domain (e.g., a large watershed) the greater the need for caution regarding weather generator treatment of spatio-temporal correlation. While impacts modeling was not the initial thrust of the NYC CCATF effort, climate scenarios for impact modeling are being developed for specific sectors (e.g., NYCDEP, 2008).
9. Is the region's climate characterized by large spatial heterogeneity?	If not, applying the delta method to a single GCM gridbox may be justifiable for many applications, as it was in NYC.
10. Are modes of variability important and predictable?	If not, the use of 30-year time slices (and the delta method) that emphasize the signal of greenhouse gases and other radiatively

important agents should be emphasized, as it was in NYC.

965

966

TABLE 3. NCAR CCSM climatology of available simulations and CCSM ensemble for the gridbox covering New York City: a) 1970-1999 hindcast; b) A1B 2080s (2070 to 2099 average) relative to the same-simulation 1970 to 1999 hindcast.

a)

	1970 - 1999 Mean temperature (°C)	1970 - 1999 Mean precipitation (cm)
CCSM Run1	9.38	98.03
CCSM Run 2	9.27	91.88
CCSM Run 3	9.67	92.08
CCSM Run 5	9.42	94.87
CCSM Run 6	9.64	95.22
CCSM Run 7	9.64	91.30
CCSM Run 9	9.68	94.69
CCSM Ensemble	9.53	94.10

b)

	2080s A1B Temperature change (°C)	2080s A1B Precipitation change (%)
CCSM Run1	3.44	2.81

CCSM Run 2	3.32	10.15
CCSM Run 3	3.03	12.44
CCSM Run 5	3.24	9.75
CCSM Run 6	2.75	9.56
CCSM Run 7	2.96	12.03
CCSM Run 9	3.01	10.36
CCSM Ensemble	3.11	9.52

973 TABLE 4. Annual and seasonal temperature (a,b,(°C decade^{-1})) and precipitation (c,d, (cm
974 decade^{-1})) trends, and 20th century (a,c) and 1970-1999 (b,d). Shown are observed Central Park
975 station data, the 16 GCM ensemble, and four points on the GCM distribution (lowest, 17th
976 percentile, and highest).

977 a)

20th century*	Min	16%	83%	Max	Ensemble	Observed
Annual	-0.03	0.02	0.12	0.17	0.07**	0.15**
DJF	-0.04	0.02	0.16	0.19	0.08**	0.20**
MAM	-0.05	-0.02	0.12	0.25	0.06**	0.18**
JJA	-0.02	0.03	0.11	0.15	0.07**	0.12**
SON	0.00	0.03	0.15	0.18	0.09**	0.08

978

979 b)

1970 - 1999	Min	16%	83%	Max	Ensemble	Observed
Annual	-0.11	0.10	0.28	0.39	0.18**	0.21
DJF	-0.47	-0.05	0.35	0.51	0.11	0.76
MAM	-0.36	-0.15	0.41	0.74	0.14	0.10
JJA	-0.01	0.13	0.29	0.44	0.20**	0.05
SON	-0.06	0.13	0.50	0.70	0.29**	-0.03

980

981

982

c)

20th century*	Min	16%	83%	Max	Ensemble	Observed
Annual	-1.22	-0.22	0.66	0.76	0.16	1.60
DJF	-0.23	-0.18	0.27	0.78	0.05	0.27
MAM	-0.27	-0.13	0.28	0.39	0.10	0.90
JJA	-0.69	-0.39	0.22	0.35	-0.07	-0.09
SON	-0.25	-0.08	0.32	0.46	0.10	0.61

d)

1970 - 1999	Min	16%	83%	Max	Ensemble	Observed
Annual	-3.52	0.02	2.05	5.73	0.87	-1.77
DJF	-3.21	-0.19	1.48	2.94	0.48	-0.48
MAM	-2.33	-1.37	1.05	1.98	-0.08	1.55
JJA	-2.08	-1.33	1.19	1.75	-0.03	-1.51
SON	-1.72	-0.55	1.89	2.93	0.48	-1.72

* Only 15 GCMs were available for the 1900-1999 hindcast.

** Trend is significant at the 99% level.

TABLE 5. Mean annual changes in temperature and precipitation for New York City.*

	2020s	2050s	2080s
Air temperature **	+ 0.8 to 1.7° C	+ 1.7 to 2.8° C	+ 2.2 to 4.2° C
Precipitation **	+ 0 to 5 %	+ 0 to 10 %	+ 5 to 10 %

* Based on 16 GCMs and 3 emissions scenarios.

** Shown is the central range (middle 67%) of values from model-based distributions; temperatures ranges are rounded to the nearest tenth of a degree and precipitation to the nearest 5%.

TABLE 6. Sea level rise projections for New York City[a]

	2020s	2050s	2080s
IPCC-based[b,]	+ 5 to 13 cm	+ 18 to 30 cm	+ 30 to 54 cm
Rapid ice-melt scenario[b,c]	~ 13 to 25 cm	~ 48 to 74 cm	~ 104 to 140 cm

[a] Based on 7 GCMs and 3 emissions scenarios.

[b] Shown is the central range (middle 67%) of values from model-based distributions rounded to the nearest cm.

[c] Rapid ice-melt scenario is based on recent rates of ice melt in the Greenland and West Antarctic Ice sheets and paleoclimate studies. See text for details.

1032 TABLE 7. Extreme Events Projections.

	Extreme Event	*Baseline (1971- 2000)*	2020s	2050s	2080s
Heat & cold events [a]	# of days per year with maximum temperature exceeding:				
	90°F (~32°C)	*14*	23 to 29	29 to 45	37 to 64
	100°F (~38°C)	*0.4*[b]	0.6 to 1	1 to 4	2 to 9
	# of heat waves per year[c]	*2*	3 to 4	4 to 6	5 to 8
	Average duration (in days)	*4*	4 to 5	5	5 to 7
	# of days per year with minimum temperature at or below 32°F (0°C)	*72*	53 to 61	45 to 54	36 to 49
Coastal floods & storms[d,e]	1-in-10 yr flood to reoccur, on average	*~once every 10 yrs*	~once every 8 to 10 yrs	~once every 3 to 6 yrs	~once every 1 to 3 yrs
	Flood heights (in m) associated with 1-in-10 yr flood	*1.9*	2.0 to 2.1	2.1 to 2.2	2.3 to 2.5
	1-in-100 yr flood to reoccur, on average	*~once every 100 yrs*	~once every 65 to 80 yrs	~once every 35 to 55 yrs	~once every 15 to 35 yrs

Flood heights (in m) associated with 1-in-100 yr flood	*2.6*	2.7 to 2.7	2.8 to 2.9	2.9 to 3.2

[a] Shown is the central range (middle 67%) of values from model-based distributions based on 16 GCMs and 3 emissions scenarios.

[b] Decimal places shown for values less than 1 (and for all flood heights)

[c] Defined as 3 or more consecutive days with maximum temperature exceeding 90°F (~32°C).

[d] Does not include the rapid ice-melt scenario.

[e] Shown is the central range (middle 67%) of values from model-based distributions based on 7 GCMs and 3 emissions scenarios.

1040 TABLE 8. Global climate model and regional climate model pairings used from NARCCAP

Global Climate Model Driver	Regional Climate Model	Combination	RCM Reference
Geophysical Fluid Dynamics Laboratory (GFDL)	Regional Climate Model Version 3 (RCM3)	RCM3 + GFDL	Pal et al., 2007
Third Generation Coupled Climate Model (CGCM3)	Regional Climate Model Version 3 (RCM3)	RCM3 + CGCM3	Pal et al., 2007
Third Generation Coupled Climate Model (CGCM3)	Canadian Regional Climate Model (CRCM)	CRCM + CGCM3	Caya and Laprise, 1999
Hadley Centre Coupled Model, Version 3 (HadCM3)	Hadley Regional Model 3 / Providing Regional Climates for Impacts Studies (HRM3)	HRM3 + HadCM3	Jones et al., 2004

1041

1042

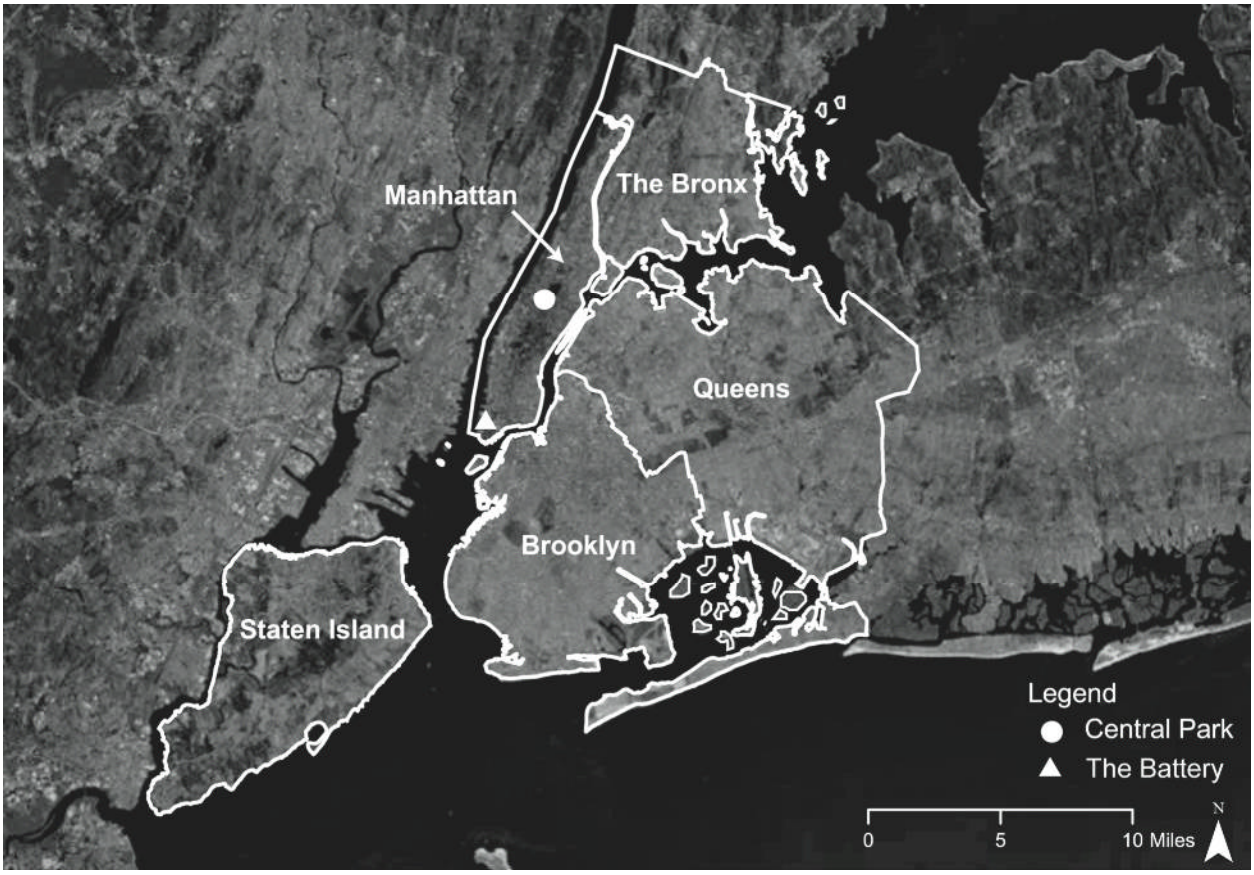

1043

1044 _

1045 Figure 1: Locations of the Central Park weather station (circle), and The Battery tide gauge
1046 (triangle), and the 5 boroughs of New York City. Source: ESRI World Imagery.
1047

1048

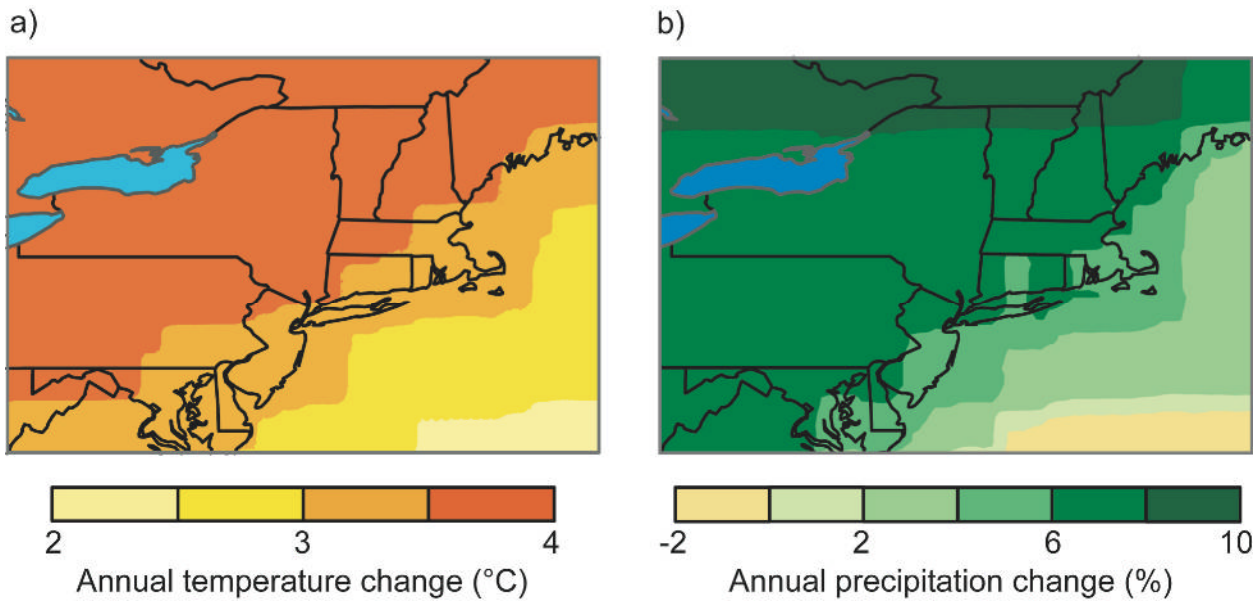

Figure 2: a) Temperature change (°C) and b) precipitation change (%) for the 2080s timeslice relative to the 1970-1999 model baseline, A1B emissions scenario and 16 GCM ensemble mean.

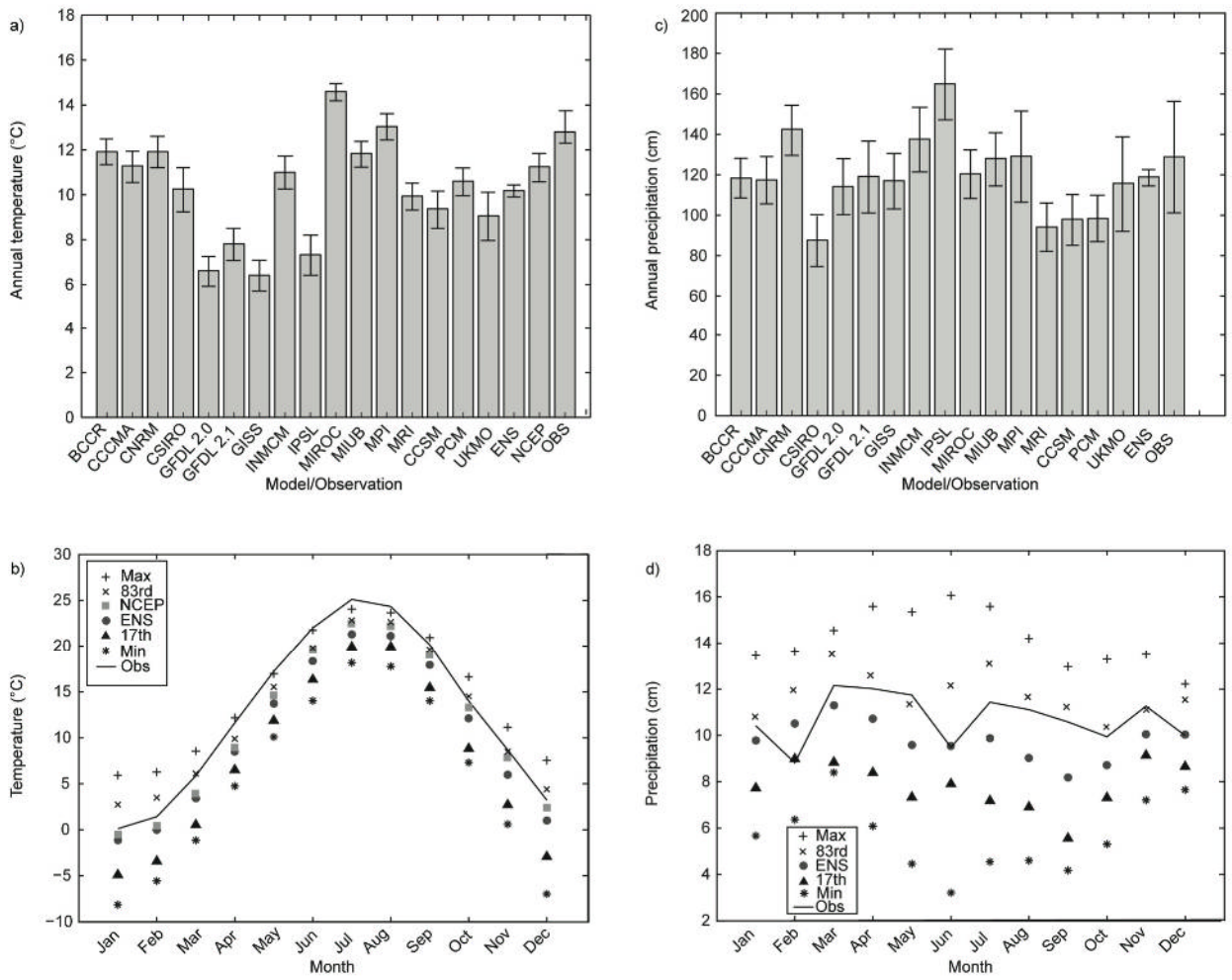

Figure 3: a) Mean annual temperature for the New York City region, (ºC), 1970-1999 in each of the 16 GCMs, GCM ensemble, Central Park station data and Reanalysis (see methods section for more information). Also shown as hash marks is the interannual standard deviation about the mean for each of the 19 products. b) monthly mean temperature for the New York City region, (ºC), 1970-1999. The two observed products, the GCM ensemble average, and four points in the GCM distribution (lowest, 17th percentile, 83rd percentile, and highest) are shown.

c) Mean annual precipitation for the New York City region, (cm), 1970-1999 in each of the 16 GCMs, GCM ensemble, and Central Park observations. Also shown as hash marks is the interannual standard deviation about the mean for each of the 18 products. d) monthly mean precipitation for the New York City region, (cm), 1970-1999. Central park observations, the GCM ensemble average, and four points in the GCM distribution (lowest, 17th percentile, 83rd percentile, and highest) are shown.

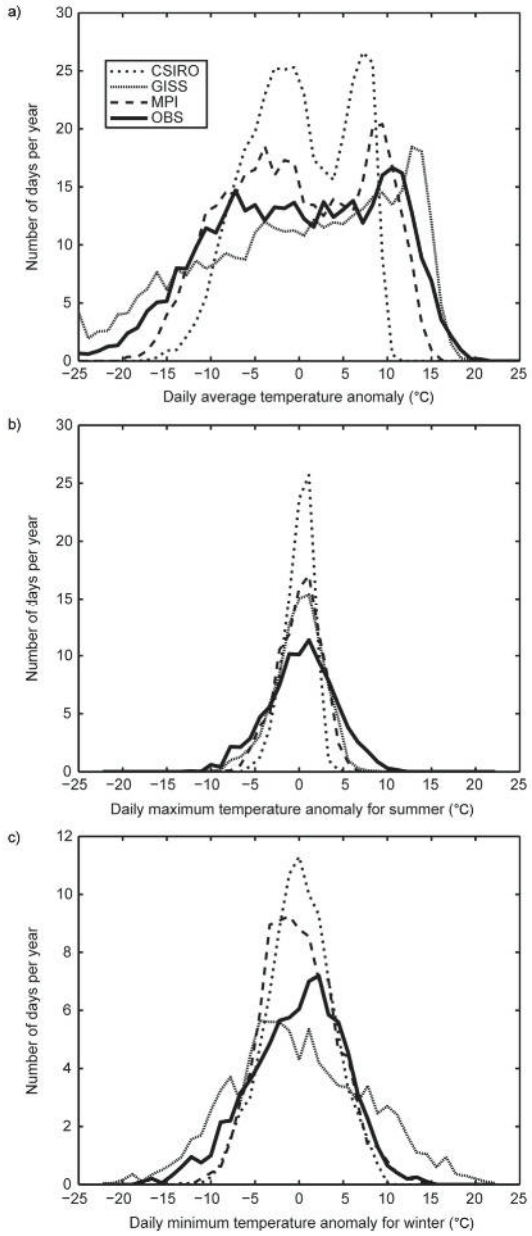

Figure 4: Daily distribution (number of days per year) of: a) all-year mean, b) summer (June-August) maximum, and c) winter (December-February) minimum temperature anomalies (ºC), 1980-1999 for Central Park observations (black line) and three GCMs (CSIRO, GISS, and MPI ECHAM5).

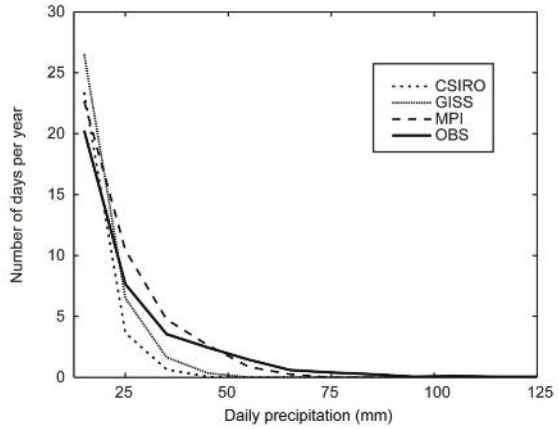

Figure 5: Daily distribution (number of days per year) of precipitation (mm), 1980-1999 for Central Park observations (black line) and three GCMs (CSIRO, GISS, and MPI ECHAM5). The first bin, containing less than 10 mm, is not shown.

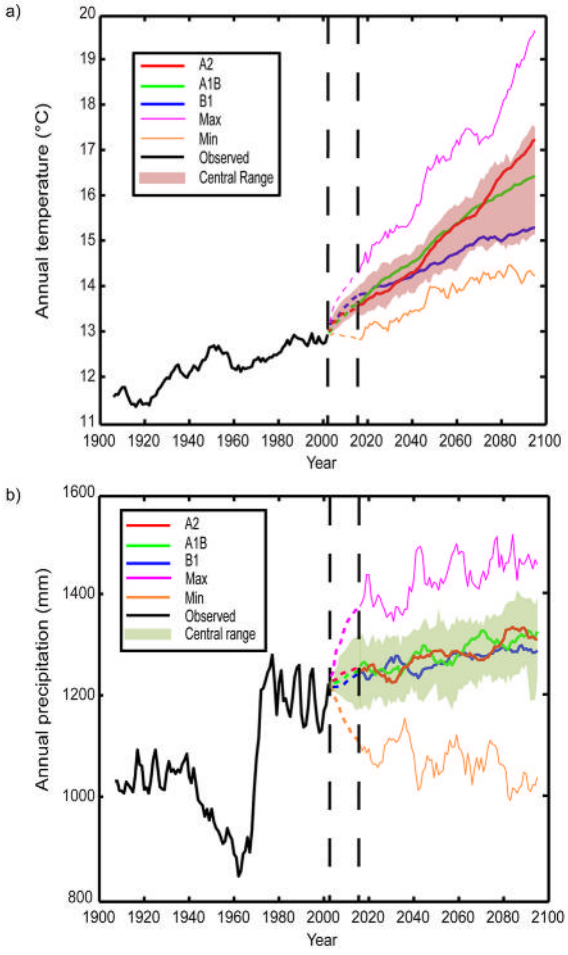

Figure 6: Combined observed (black line) and projected: a) temperature (ºC) and b) annual precipitation (mm). Projected model changes through time are applied to the observed historical data. The three thick lines (red, green, and blue) show the ensemble average for each emissions scenario across the 16 GCMs. Shading shows the central 67 % range across the 16 GCMs and 3 emissions scenarios. The bottom and top lines, respectively, show each year's minimum and maximum projections across the suite of simulations. A ten-year filter has been applied to the observed data and model output. The dotted area between 2003 and 2015 represents the period that is not covered due to the smoothing procedure.

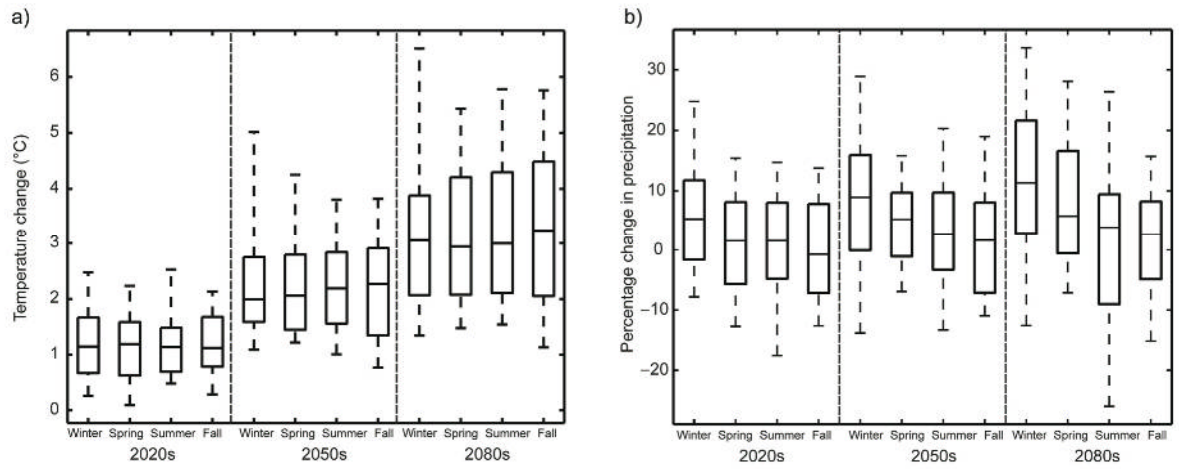

Figure 7: Seasonal a) temperature change (ºC) and b) precipitation change (%) projections, relative to the 1970-1999 model baseline, based on 16 GCMs and 3 emissions scenarios. The maximum and minimum are shown as black horizontal lines; the central 67% of values are boxed, and the median is the thick line inside the boxes.

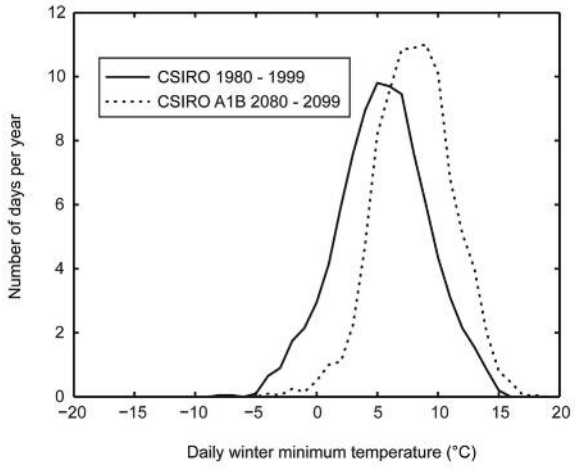

Figure 8: Daily distribution (number of days per year) of winter (December-February) minimum temperature anomalies (ºC), for the New York Metropolitan Region in the CSIRO GCM. Black line, 1980-1999 hindcast; dotted line, 2080-2099 A1B scenario.